Power System
Modelling and Analysis

An Engineering Internship at Fortescue Metals Group

Prepared by: Jessica Mattingley

Submitted to the School of Engineering and Information Technology, Murdoch University

Academic Supervisor: Dr. Gregory Crebbin

Industry Supervisor: Cobus Strauss

24th November 2014

Abstract

To fulfil the requirements of the Bachelor of Engineering at Murdoch University, students are required to undertake either a research project or internship project. This final year thesis project was carried out during an internship placement at Fortescue Metals Group ("Fortescue"). The project involved the modelling and analysis of a new power system at one of Fortescue's mine sites in the Pilbara region of Western Australia.

Power systems are modelled for the purpose of analysing system safety, reliability and efficiency. The process that engineers take to ensure power systems have these qualities in the design phase is greatly simplified by modelling. The modelling is carried out using specialised power system analysis tools in order to simulate the steady-state and transient operating conditions that system components are likely to be subjected to.

The power system modelling at Fortescue was carried out in the preferred modelling software, PowerFactory by DIgSILENT. The studies that were undertaken for analysis were Load Flow, Short-Circuit and Motor-Starting Studies, with an additional task of assessing the coordination of protective devices. The Load Flow study was carried out for the normal operation of the system, where the system is running at maximum demand. The Short-Circuit study scenarios included the maximum and minimum prospective fault currents during three-phase short-circuits and single-phase to ground short-circuits. The Motor-Starting studies were carried out on the maximum motor loads connected to each substation. The methodology and techniques used to conduct these studies are outlined in the report.

The results indicated that the system components were adequately rated in order to safely and reliably supply power to the various loads. Equipment ratings were not exceeded in normal operation of the system, or throughout any of the short-circuit fault scenarios. The studies illustrated that motors could successfully start-up without damaging equipment due to inrush currents, and the protection settings were all adequately coordinated. The detailed analysis of these results is carried out throughout this internship report.

Acknowledgements

I would like to thank Fortescue Metals Group for demonstrating such great support for young professionals entering the industry. Thank you to Mark Azzopardi for the fantastic opportunity to undertake an internship within your team.

I would like to thank my industry supervisor, Cobus Strauss, for allowing me the opportunity to carry out the internship under your supervision. I would also like to acknowledge Ashley Edlington and Nicholas Sweetman for your support and guidance over my time at Fortescue so far. Your continued support is much appreciated and the knowledge I have gained from you all throughout my internship is invaluable.

I would like to thank Dr. Gregory Crebbin for your assistance and helpful feedback throughout this project and the many other projects throughout my degree at Murdoch.

Thank you to all of my peers who have become friends along the way. University would not have been the same without you.

And last but certainly not least, I would like to thank my family and friends. Your ongoing support is what has made this all possible.

Thank You.

Table of Contents

List of Equations

List of Figures

List of Tables

List of Abbreviations

Abbreviation	Definition
a.c.	Alternating Current (also commonly abbreviated to AC)
AS	Australian Standard
AS/NZS	Australian and New Zealand Standard
Cu	Copper
DOL	Direct-on-Line
FMG	Fortescue Metals Group
HV	High Voltage: Voltage exceeding 1000V a.c.
IEC	International Electrotechnical Commission
kA	Kilo Amperes
kV	Kilo Volts
kVA	Kilo Volt Amperes
kW	Kilo Watts
LV	Low Voltage: Voltage exceeding 50V a.c. but not exceeding HV
MCC	Motor Control Centre
ms	Milliseconds
mtpa	Million tonnes per annum
MVA	Mega Volt Amperes
MW	Mega Watts
OPF	Ore-Processing Facility
pu or p.u.	Per-Unit
PVC	Polyvinyl Chloride
rms	Root-Mean-Square
rpm	Revolutions per minute
SLD	Single Line Drawing
SS	Soft-Starter
VSD	Variable Speed Drive
XLPE	Cross-linked Polyethylene

Page intentionally left blank.

1 Introduction

1.1 The Internship

To fulfil the requirements of the Bachelor of Engineering degree at Murdoch University, students are required to undertake either a research thesis or an internship in a relevant industry placement. The engineering internship provides students with a unique opportunity to gain invaluable knowledge and experience that complements the engineering degree. This internship was carried out at Fortescue Metals Group Limited ("Fortescue") in the corporate Engineering department over the period of July to November 2014. The intern was involved in various projects in the electrical engineering team with the main project of modelling and analysing a new power system at one of Fortescue's mine sites. This allowed the intern to apply the skills learned at university in a practical setting and provided exposure to engineering practice, design, operations, management and reporting in a professional sense. Throughout the course of the internship, the intern was required to submit a project plan and progress report which allowed project tasks to be completed in a timely manner. In addition to these assessment items, the intern was required to submit a formal report and presentation on the project work carried out during the internship at Fortescue. This report details the main project that the intern was directly responsible for in the placement at Fortescue.

1.2 Fortescue Metals Group Limited

Fortescue is a successful Australian mining company that has become the world's fourth largest iron ore producer since its formation in 2003. The economic growth in China, South-East Asia and India has facilitated Fortescue's expansion and success in the iron ore market. First construction began in the Pilbara region of WA on its flagship mine Cloudbreak in 2006, while also constructing a 256km rail line from Cloudbreak to Port Hedland and the world class ship-loading facilities at Port Hedland. The first production from Cloudbreak and cargo shipment from Port Hedland was in 2008. Currently Fortescue has four operating mines and ore-processing facilities as shown in Figure 1 and produces iron ore at a rate of 155 million tonnes per annum (mtpa). The latest development for Fortescue is the Iron Bridge project where North Star is the first mine being developed and will be completed in 2 stages. Fortescue maintains various power stations and distribution networks at all of its mine sites and is in the process of building and maintaining the models for these power systems in DIgSILENT's PowerFactory.

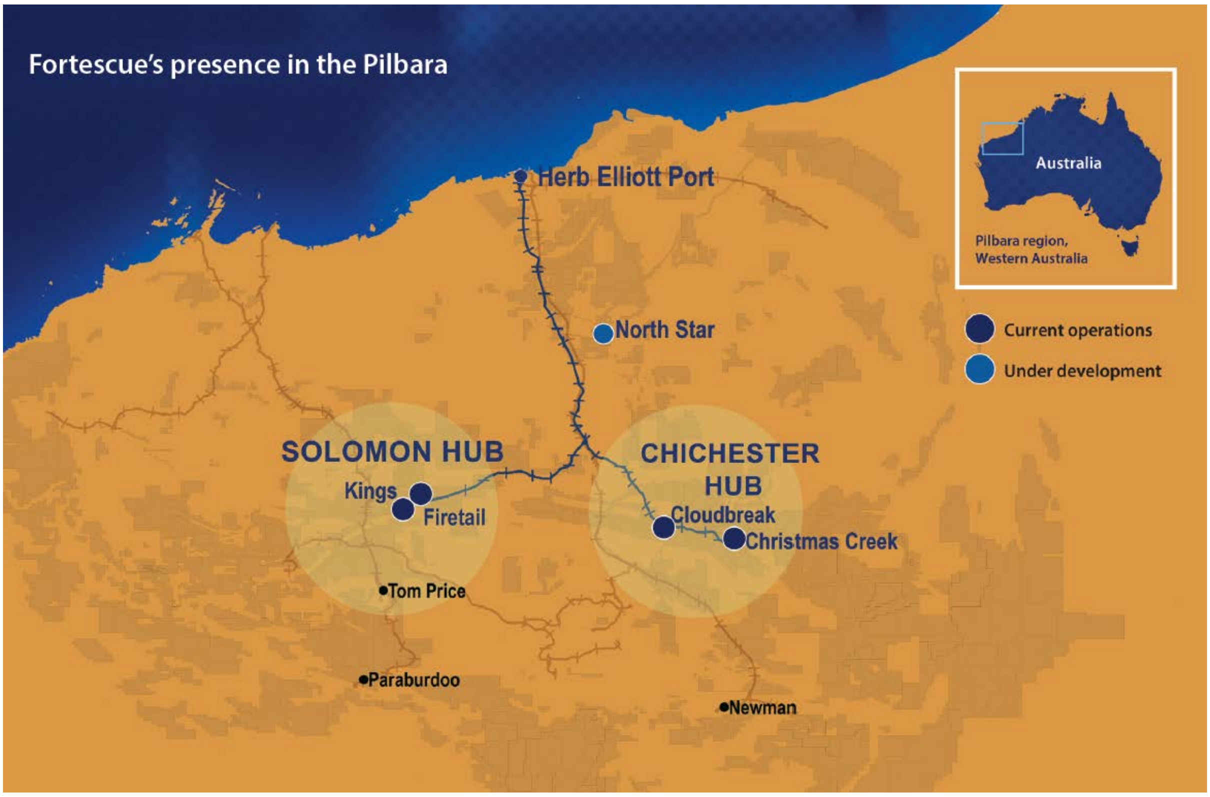

Figure 1: Operations Map [1]

1.2.1 North Star

Fortescue is expanding its operations into a new joint venture project known as Iron Bridge which is located approximately 120km SSE of Port Hedland. Iron Bridge is comprised of the North Star and Glacier Valley iron ore deposits with a combined iron ore resource of 5.2 billion tonnes. A Fortescue shareholder announcement states the joint venture participants are FMG Magnetite Pty Ltd (69%) and Formosa Steel IB Pty Ltd of Taiwan (31%), where FMG Magnetite Pty Ltd is a joint venture between Fortescue (88%) and China's Baosteel (12%) [2]. The announcement also states that Stage One of the North Star development will see production of 1.5mtpa of 66% Fe mHematite ore while Stage Two will produce 9.5mtpa of 68% Fe magnetite concentrate. Throughout Fortescue's mine sites there are several high voltage distribution networks fed from their onsite power stations. The facilities at North Star Stage One will be powered from a 16 MW stand-alone power station, distributed via an 11 kV network to five substations. This is shown in Figure 7 and Figure 8 for the single line drawing and the PowerFactory model representation respectively. If the Stage Two development is approved, the facilities will be supplied by an additional power station and distribution network. This internship project is focused on the development of the PowerFactory model for the North Star Stage One power system.

2 Project Description

Power systems must be analysed in detail throughout all stages of the design, commissioning and operation of the network. The studies that can be carried out using specialised software give an overview of how the system will respond under normal operating conditions and in transient fault conditions. In order to meet regulatory requirements under the WA Electrical Requirements, those intending to install a HV power system must prove its reliable and safe operation with a HV Submission before energizing the system [3]. The power system studies that can provide evidence of potentially safe and reliable operation include load flow, short-circuit, protection coordination, and motor starting studies.

Load flow studies provide a means to calculate the voltages and currents in different parts of the network, and assist in the design and selection of adequately rated equipment. In PowerFactory, load flows can be carried out using the in-built load flow function which provides information on the power loading and power factor, as well as voltages and currents in all areas of a power system. The load flow scenario that will be examined is the normal operation at maximum demand of the system, which is when there is 14MW of generation online, with 2MW standby.

Short-circuit studies are essential to determine the behaviour of a power system under fault conditions. It is a time intensive process to carry out short circuit studies by hand, and it is far more effective to do this using capable software such as PowerFactory. The studies give approximate prospective fault levels in all areas of the network and allow for the equipment to be rated to handle the expected currents without damage. The standards that are followed throughout the short-circuit studies will be IEC60909 and AS3851. Three-phase short circuits and single-line to ground short circuit studies are carried out at all buses. The system protective devices are modelled in PowerFactory and assessed for correct coordination.

The final studies that are carried out on the system are motor starting studies. These studies are useful in determining the effect that the initial start-up current has on the system in terms of voltage drop and equipment loading. If the equipment is not rated adequately, there is the risk of damage due to thermal overloading of equipment. If equipment is subjected to currents that are too high and for too long, then reliability and safety of the network are compromised. In PowerFactory, motor starting studies are relatively simple and provide the user with a graphical representation of the effects on the system.

Ultimately Fortescue will maintain the models for all of their site power systems, which will reduce costs involved in both operational maintenance and expansion works as design studies can be performed in-house as opposed to engaging external consultants. The North Star power system has been modelled and analysed by the engineering agency Petro Min Engineers (PME) prior to this internship commencing, and therefore this analysis serves as a validation of the previous studies.

3 Power System Modelling

3.1 Background

Modelling is an important aspect in the design and engineering of all power systems. The analysis of power systems is required in engineering practice in order to determine the steady state and transient operating conditions that are needed for safety and reliability. Modelling software is utilised in which the system is represented graphically and analysed by mathematical algorithms. It is important to include as much information for on electrical equipment as accurately as possible. Various studies can then be carried out in order to determine operating limits and loadings, system efficiency and stability and determine optimal protection settings for equipment.

3.2 PowerFactory Software

The software that has been utilised throughout this power system analysis is PowerFactory by DIgSILENT GmbH. PowerFactory is one of the leading power system study packages in the market today, and is widely used throughout industry. The version that Fortescue is currently using is PowerFactory 14.1.4 (x64), which has a wide range of functions that exceed the scope of this project. In the past, Fortescue have engaged DIgSILENT to model their site power systems, however North Star is being modelled in-house as part of ongoing cost improvements to the business. Fortescue uses PowerFactory to maintain models of their site power systems and run studies when necessary for expansion planning.

3.3 Resources

There are various resources that are utilised in order to build the model with the most accuracy possible. As North Star is a site currently under construction rather than an existing site, there is more information that is readily accessible from different sources. In the past, when the modelling of Fortescue power systems has been undertaken for the purpose of adding to the internal collection of models, there have been significant portions of equipment information that were not available. In those cases, site visits were the primary method of information collection. However this is not an issue for North Star. The resources that are available are as follows:

- Fortescue Drawing Database
- Overall Single Line Drawing
- Manufacturer’s Data Sheets
- Cable Schedule
- Cable Sizing Report
- Electrical Load List

3.4 Assumptions

There are several assumptions made throughout the entirety of the modelling in order to allow the successful progression of the modelling process. These assumptions are outlined in the relevant sections where the assumptions are implemented.

3.5 Equipment Parameters

3.5.1 Synchronous Generators

The North Star power station is comprised of five three-phase 2000kVA and eight 1250kVA Cummins-Stamford diesel generators with a combined capacity of 16MW. The rated voltage of 415V and rated frequency of 50Hz comply with the Fortescue Standard Engineering Specification for Electrical Design Criteria 100-SP-EL-0001 [4]. These generators have been modelled in PowerFactory as synchronous machines that are dispatched according to their active power rating. The power factor is chosen for the mode of local voltage control which keeps the generators operating at their rated power factor of 0.8 lagging.

As can be seen in the site single line drawing (SLD) in Appendix A, these generators are connected to the main 11kV switchboard SB-001 through 2MVA and 2.5MVA step-up power transformers. The 1250kVA generators are paired and connected to a 2.5MVA transformer, and the 2.5MVA transformers are paired again before feeding into SB-001 via a load break switch. The 2000kVA generators are directly connected to 2MVA transformers, which are then paired and connected to SB-001 via a load break switch. One remaining 2000kVA generator is connected directly to a 2MVA transformer and to SB-001 via a load break switch. A station controller has also been modelled to control the voltage at the 11kV bus to be 1.0p.u. This causes the generators to operate at a voltage slightly higher than their nameplate rating in order to overcome the voltage drop between the generators and SB-001.

The relevant parameters for the generators have been extracted directly from their respective data sheets and are given in Table 1.

Table 1: Synchronous Generator Input Data [5] [6]

Description	1250kVA Values	2000kVA Values
Active Power (MW)	1.0	1.6
Nominal Apparent Power (MVA)	1.4	2.2
Nominal Voltage (kV)	0.415	0.415
Frequency (Hz)	50	50
Power Factor	0.8 lagging	0.8 lagging
Synchronous Reactance Xd (p.u)	3.02	3.20
Synchronous Reactance Xq (p.u)	1.95	2.06
Subtransient Reactance Xd” (p.u)	0.14	0.13
Transient Reactance Xd’ (p.u)	0.18	0.18
Zero Sequence Reactance X0 (p.u)	0.02	0.03
Neg. Sequence Reactance X2 (p.u)	0.19	0.18
Leakage Reactance XL (p.u)	0.03	0.03
Stator Resistance (ohms)	0.0016	0.0008
Stator Resistance (p.u)	0.01300624	0.01021919
X/R Ratio	10.76406	12.72116
Transient Time Const. Td’ (s)	0.13	0.16
Subtransient Time Const. Td” (s)	0.01	0.01

The Cummins KTA50-G3/Stamford PI734B 1250kVA generators have a kVA base of 1400 for its reactance values and the Cummins QSK60-G4/Stamford PI734G 2000kVA generators have a kVA base of 2200 for its reactance values.

The zero- and negative-sequence resistive components were not specified in the data sheets and have been left at their default value of 0 in PowerFactory. The only remaining parameters that are not explicitly shown in the data sheet are the stator resistance in per unit or the X/R ratio. Entering either of these values into PowerFactory automatically fills the other with a value, as they are related. For example, the 1250kVA generator main stator resistance is 0.0016 ohms per phase, which is found to be:

Equation 1: Stator Resistance (p.u)

$$R\ (p.u.) = \frac{R_{stat}}{Z_{base}}$$

$$R\ (p.u.) = \frac{0.0016\ ohms}{\frac{V_{base}{}^{2}}{S_{base}}}$$

where

V_{base} is the generator voltage: 415V

S_{base} is the kVA base rating for the reactance values: 1400kVA

therefore

$$R\ (p.u.) = \frac{0.0016\ ohms}{\frac{415^2}{1400000}} = 0.01300624$$

Putting $R\ (p.u.) = 0.01300624$ into PowerFactory gives the X/R ratio = 10.76406 as it uses the subtransient reactance of Xd" = 0.14 to compute the X/R ratio. The same method has been used for the 2000kVA generators.

3.5.2 Transformers

Throughout the entire North Star power system there are just seven different transformer types for the 19 transformers installed on site, which simplifies modelling considerably. Table 2, Table 3 and Table 4 illustrate the simulation relevant information entered into PowerFactory from the manufacturer's data sheets. The rated power, rated voltage, vector group, copper losses and positive sequence impedance parameters were taken from the data sheets, while the remaining input parameters were calculated or assumed. Each transformer also has tap changing capabilities when needed with tap settings of 2 × ± 2.5% on the HV winding, excluding the earthing transformer.

The rated power and rated voltages of each of the transformers can be seen in the North Star SLD in Appendix A. The power station supplies power at 415V to the main 11kV switchboard SB001 through the 2MVA and 2.5MVA step-up transformers. The auxiliary loads for the power station and SB001 are supplied via a 500kVA step down transformer. The 11kV switchboard is earthed through a 100A earthing transformer. Outside the power station, there are five 415V motor control centres (MCCs) supplied by the 2.5MVA step down transformers. The final two transformer types are used for three high voltage motors supplied through three different 3-winding transformers.

The vector group of the transformer determines whether there is a phase shift between the primary and secondary side currents and voltages. The vector group notation uses upper case letters for the HV winding, lower case letters for the LV winding and the digit indicates the phase shift. The phase shift is described using numbers 1-12 as on a clock with 1 being -30°, 6 being 180° and 11 being +30°. For example, for the vector group Dyn11, the HV side is delta connected, the LV side is star-neutral connected and the phase-to-neutral voltages on the star side lead the delta voltages by 30° [7]. The vector group also determines which zero sequence currents will flow. The zero sequence current will only flow in a star-connected set of impedances if the neutral point is earthed either directly or through earthing impedance. For a delta connected set of impedances the zero sequence current can only flow inside the delta by mutual coupling, and will not exit through the output terminals into the system [7].

The positive sequence impedance and the copper losses of each transformer are used to calculate the X/R ratio in PowerFactory. The resistive component of the impedance is calculated by the formula

Equation 2: Copper Loss

$$Copper\ Loss = I^2 R$$

where

Equation 3: Three-Phase Relationships

$$I = \frac{S_{3\varphi}}{\sqrt{3} V_{LL}}$$

and the reactance is then computed by the simple Pythagoras rule with Z and R being the known variables. The X/R ratio is important for power system modelling as it determines the magnitude of the asymmetrical fault current at different areas of the system. The higher the X/R ratio, the slower the decay rate of the DC component of the short-circuit current, and the higher the peak fault current that the system and protective devices see and are required to interrupt [8].

The zero sequence impedance is not typically specified in manufacturer's data and is the only parameter that has been assumed in modelling the transformers. It has been assumed that the zero sequence impedance is 85% of the positive sequence impedance [9] which was recommended in a DIgSILENT technical reference for transformers.

Table 2: Two-Winding Transformer Input Parameters [10] [11] [12] [13]

Transformer I.D.	Rated Power	Rated Voltage	Vector Group	Copper Losses	X/R Ratio	Pos. Seq. Impedance	Zero Seq. Impedance
	MVA	kV		kW		%	%
TF-01	0.5	11 / 0.415	Dyn0	4.5	4.3305	4	3.4
TF-02 : TF-07	2.5	11 / 0.415	Dyn11	26.719	7.1231	7.6875	6.15
TF-11 : TF-15	2	0.415 / 11	Dyn11	17.1	7.2412	6.25	5.3125
TF-16 : TF-19	2.5	0.415 / 11	Dyn11	22.43	6.8940	6.25	5.3125

Table 3: Earthing Transformer Input Parameters [14]

Transformer I.D.	Rated Voltage	Rated Current (Ie=3*I0)	Zero Sequence Resistance
	kV	A	Ohm
TF-20	11	100	190.52

Table 4: Three-Winding Transformer Input Parameters [15] [16]

Trans-former I.D.	Rated Power HV/MV/LV	Rated Voltage HV/MV/LV	Vector Group	Copper Losses	X/R Ratio	Pos. Seq. Impedance HV-MV / MV-LV / LV-HV	Zero Seq. Impedance HV-MV / MV-LV / LV-HV
	MVA	kV		kW		%	%
TF-21 : TF-22	3.554/1.777/1.777	11/1.903/1.903	D0y11d0	26	5.0275	7.5/7.5/7.5	6.375/6.375/6.375
TF-23	2.4/1.2/1.2	11/2.2/2.2	D0d0y11	25.7029	3.02/3.20/3.03	6.81/7.17/6.84	5.788/6.094/5.814

The three-winding transformers TF-21, TF-22 and TF-23 are being used to supply large VSDs that require 2 inputs to drive large high voltage motors. To model the three winding transformers connecting to a single VSD/motor load in PowerFactory, the load was required to be split into two to allow the simulation to run. The software gives an error if the two lower voltage windings of the transformer are connected to the same bus.

3.5.3 Cables

The cables have been modelled according to the North Star project cable sizing calculations and cable schedule, the relevant cable data sheets, and AS3008. The following information is needed for each cable to successfully perform studies in PowerFactory:

- Cable Length
- Rated Voltage
- Rated Current
- Nominal Frequency
- Phases/Neutrals
- Conductor Material
- Resistance per length 1,2-Sequence and Zero Sequence
- Reactance per length 1,2-Sequence and Zero Sequence

And optional for further analysis:

- Max Operational Temperature and Max End Temperature
- Rated Short-Time (1s) Current

The manufacturer's data sheets were available for the high voltage cables, however there were no data sheets available for the low voltage cables. Therefore the reactances and resistances for the low voltage cables were found from AS3008 Tables 31 and 37 respectively. Table 12 and Table 13 in Appendix B show the conductor types that have been modelled in PowerFactory and the locations and lengths of these cables. It should be noted that the cables on the low voltage side of transformers TF02, TF03, TF04, TF05 and TF07, and the cables feeding the loads from each of the MCCs have been left out of the model. This is due to the information for these cables being unknown, and omitting these cables will not have a significant effect on the results. The effect will not be significant as these cables are typically very short and, as such, the impedances that they would add to the circuit relative to all other system impedances are very small. As a result of omitting these cables, the short-circuit fault currents at the MCCs will be higher than they would be in practice due to the before mentioned cables impedances not being included in the model.

3.6 Electrical Loads

The loads have been modelled based on an electrical load list compiled by the team within Fortescue that is managing the North Star project. This electrical load list gives information on the installed kW rating of the load and whether the load is duty or standby. The summary of this list is given in Appendix B where the total load on each MCC or HV motor is given. While the load list has been compiled based on the design for the North Star process plant, detailed information is not available. Due to not having nameplate data for every load on site, some assumptions must be made in order to move the model into an operational state. These assumptions will be outlined in the following sections where applicable.

A combined diversity/load factor of 70% has been applied to the loads of MCC02, MCC03, MCC05 and MCC07 in order to provide a more realistic expectation of power consumption in the network. MCC04 has a diversity factor of 60% based on advice of the supervising electrical engineer for North Star, as this area of the plant is typically operated in two sections and therefore 70% is too excessive. A load factor is typically used when a motor is not running at full capacity, and a diversity factor is used to account for not all equipment being on at the time of peak load [17]. This is important when modelling a power system as not all loads will be operating at full load simultaneously, and this must be represented in order to study the system as accurately as possible.

Power systems operate with hundreds of electrical loads and to represent each and every one in PowerFactory would be unnecessary and time consuming. Each load is not modelled separately as it gives little to no extra information about the system compared with modelling lumped loads [18]. All HV and LV loads have been captured down to the 415V/240V level. Modelling smaller loads than this will provide only marginal extra information about the operation of the system.

The breakdown of loads on each LV busbar or MCC is as follows:

- Largest Direct Online (DOL) Motor
- Lumped DOL Motors
- Lumped Soft Starter (SS) Motors
- Lumped Variable Speed Drive (VSD) Motors
- Lumped Static Loads

Table 14 and Table 15 in Appendix B illustrate all of the loads that have been modelled with the applied diversity factors. A brief description of the input settings required for each load type is presented below.

3.6.1 Static Loads

General or static loads are non-rotating loads and are modelled by a simple element that only requires information for the power rating and voltage set-point. The voltages of the static loads are set to 1.0pu and the power factor is assumed to be 0.9 lagging due to the wide variety of lighting and small power loads [19].

3.6.2 DOL Motors

Direct online motors have been modelled using the asynchronous machine element in PowerFactory. The largest DOL motor on each bus has been modelled separately and all remaining DOL motors have been aggregated into a lumped motor load. The largest DOL motor must be modelled independently of the rest so that motor starting studies can be performed and protection settings can be graded correctly. This will be carried out in later sections of the report. The asynchronous machine element requires the user to enter values for the bus type, active and reactive power, mechanical power, power factor, rated voltage, frequency, number of pole pairs, winding type, locked rotor current ratio and X/R ratio. The stator reactance and torque at stalling point settings are left as their default values of 0.01pu and 4.824 respectively due to lack of information. All other elements within the settings are either greyed out due to the parameter relying on other entries to give a calculated value, or are not crucial to the power system studies.

- The input mode is assumed to be the “slip-torque/current characteristic” as this method relies only on the user entering the rated mechanical power, power factor and nominal speed in order to calculate the equivalent circuit parameters by conversion. This input mode is chosen over the “electrical parameter” method because the latter method requires the specification of the resistances and reactances of the equivalent circuit characteristics for the motor, which are unknown.
- The bus type is selected from two options: AS and PQ. The AS “slip iteration” method is used when equivalent circuit characteristics are known about the motors being modelled and provides a more accurate solution to the load flow calculations [20]. The PQ bus type requires only the active power and reactive power to be specified, which assumes a motor power factor independent of the bus voltage. The PQ method has been used throughout the North Star model due to the limited load information available.
- The power factor that has been applied for the DOL motors is assumed to be 0.85 lagging based on averages taken from ABB low voltage motor data sheets [21]. Typically, smaller

motors have lower power factors, and larger motors have higher power factors in the range of 0.8-0.9 [22].

- The mechanical power is entered as per the installed kW rating in the electrical loads list.
- All of the DOL motors represented in the North Star model are rated at 415V as they are fed via the 11kV/0.415kV transformers. Typically, motors at Fortescue are rated for 400V as per Fortescue Specification 100-SP-EL-0001, however the rated transformer secondary voltage was increased from 400V to 415V in the early design stages due to the prospective fault current contribution from the motors being too large.
- The rated frequency of all motors is assumed to be 50Hz to comply with Fortescue Low-Voltage Induction Motor Specification 100-SP-EL-0013 [23].
- The number of poles has been assumed to be 4, or alternatively 2 pole pairs, as this is typical of most motors in industry. This corresponds to a synchronous speed of 1500rpm using the formula:

Equation 4: Rotor Speed

$$Speed = \frac{120 \times Freq}{No. of\ poles}$$

Upon choosing 2 pole pairs in PowerFactory, the rotor speed is given as a calculated value of 1485.7rpm using the default motor model characteristics.

Therefore

Equation 5: Motor Slip

$$slip = \frac{n_s - n_{rot}}{n_s}$$

$$slip = \frac{1500 - 1485.7}{1500}$$

$$slip = 0.00953 \ \approx 0.01 \ or \ 1\%$$

where

n_s is the synchronous speed of the magnetic field

n_{rot} is the rotor speed

- The winding type has been chosen to be delta wound as per Fortescue Specification 100-SP-EL-0013 which states that motors larger than 2.2kW shall be delta connected.
- The locked rotor current ratio is assumed to be $\frac{I_{LR}}{I_{nom}} = 5$, and the X/R ratio is assumed to be $X_M/R_M = 1/0.42$ as per AS3851 page 37. These values are given for low voltage motors that have been grouped into an equivalent motor load including their connection cables, for simplification [24].

3.6.3 SS Motors

Motors connected to the power system through soft starters (SS) have a significantly lower impact on the system during start-up conditions than DOL motors. The soft starter decreases the start-up torque and current surge by reducing the applied voltage and incrementally increasing it to rated voltage through semiconductor circuitry. Motors connected to the system through soft starters can be modelled in the lumped DOL motor loads, however for simplicity they have been modelled separately. Although the starting characteristics of the soft starter fed motors are different to the DOL motors, they both act the same under normal steady state operation. Similarly, under short circuit conditions, the soft starters do not impede the motors from contributing current to the fault much the same as DOL motors. All settings discussed in section 3.6.2 for DOL motors are replicated in the SS-fed motor loads.

3.6.4 VSD Motors

Variable Speed Drives (VSDs) have been implemented in the North Star power system wherever it is necessary to have control over the speed of the motor for certain applications. VSD fed motors act much like a static load under steady-state operating conditions, and do not provide any short-circuit current in fault conditions. Therefore VSD motors are modelled as general static loads in PowerFactory but are kept separate from normal static loads due to their different power factors. VSDs typically have a power factor of 0.93 lagging, whereas general loads typically have a power factor of 0.9 lagging [25] .

3.7 Validation

Various measures were taken to ensure the accuracy of the data in all aspects of the modelling process, however there is always the chance of human error or the data being incorrect for the particular application. The model and the results are only as accurate as the information that is put into it. Throughout the modelling process, the equipment parameters were intermittently reassessed according to their respective data sheets to determine whether corrections were necessary. By doing this, there were several occasions where additional parameters were added to the equipment models and helped to improve the overall accuracy of the model. In the external consultant's (PME) model, there were various extra assumptions made due to the exact equipment information being unknown, as the vendor for the equipment had not been selected at the time. For example, the power station step-up transformers had the resistance and reactance assumed based on X/R = 10 for transformers, as recommended in the standard AS3851. Therefore, while the results of PME's studies were referred to for comparative purposes, the differences could be due to these various assumptions. Validation of the results was also undertaken by comparing them to the expected results from various hand calculations of short-circuits. While the model will be more accurate than the hand calculations if the data is all correct, the hand calculations were useful to determine whether there were any significant problems with the data entered.

4 Load Flow Analysis

4.1 Background

Load flow studies are performed for many reasons, and are useful to analyse both operational power systems and future or expanding power systems. With a power system simulator it is very simple to perform many different load flow studies for different operating scenarios. The purpose of load flow studies is to determine voltage levels, check active and reactive power flows and assess the loading of equipment under steady-state conditions. All power systems must operate within specified limits in order to meet regulatory requirements for safe network operation.

The steady state voltages throughout the system can be determined under different operational scenarios by performing load flow studies. Nominal voltages in low voltage supply systems in Australia must be within +10% to -6% of 230/400V as per AS3000. This is to prevent damage to electrical equipment that has been designed and rated according to the standard. The low voltage installations at North Star are rated for 415 volts which is within the limit at +3.75% of 400V. The Fortescue Specification 100-SP-EL-0001 states that the normal operating voltage range shall be limited to ± 5% for both high voltage and low voltage installations. AS3000 also states that the voltage drop from the point of supply of the low voltage installation to the load must not exceed 5%.

The active and reactive power flows in a system are important and provide important information about the design of the system. The power flows are analysed to determine whether there is adequate generation to meet the requirements of the system, to assess whether the power factor is within the desired region, and to give an indication of the power losses. The Fortescue Specification 100-SP-EL-0001 states that the power factor target for supply quality is 0.95 lagging. Many different studies can be run for various typical operating scenarios, such as when certain generators are being serviced or a line is taken out of service. The load flow studies can be performed to identify the need for capacitive VAR support or voltage regulation.

Load flow studies also provide important information on the loading of electrical equipment throughout the system. It is recommended that equipment such as transformers and cables are loaded at less than 80% and as such this will be the loading threshold for verification throughout the model. The generator loadings are also of interest to determine whether they are operating at high efficiency, as the 1400kVA and 2200kVA generators operate most efficiently at 68% and 65% loading respectively, as shown in Appendix B.

4.2 Methodology

AC Load Flow studies are carried out using iterative mathematical methods to solve the power flow equations. These methods begin the simulation with an initial solution and perform a series of iterations in order to converge on the true solution [26]. The calculations determine the voltage magnitude and angle of the nodes, and active and reactive power flows in each branch, where the network nodes are represented by specifying two of these four parameters [20]. PowerFactory uses the Newton-Raphson algorithm with a choice of the “Current Equations” or “Power Equations, Classical” method of calculation. In this case both methods produce the same results and converge within three iterations, with the current equation method usually converging in two iterations. The maximum number of iterations was specified as 25 with the maximum acceptable load flow error for nodes set at 0.01kVA and for model equations as 0.1%.

The active power control of the system is “As Dispatched”, which allows the system to balance the generation over all generators using the power balancing method of “Distributed Slack by Generation (Synchronous Generators)”. This option is chosen over the typically used “Reference Machine” method, as the generators were not all balanced using the reference machine method. A station controller was implemented to control the voltage at the 11kV switchboard SB001 to be 1.0p.u. This is typically what is implemented in practice, where generators are connected one by one in order to synchronise and load share.

4.3 Results

There are many different operating scenarios that can be assessed by carrying out load flow analyses. The load flow case of most importance, and the one that has been performed in this analysis, is the normal proposed operation of the system. This load flow was performed at maximum demand of the system, with six 1MW generators and five 1.6MW generators running to supply 14MW. The maximum demand was assumed to be when the diversity factors stated in Section 3.6 are applied.

The following results are presented based on the verification limits of ± 5% for the system voltages and 80% loading of equipment. The voltages throughout the system remain within the specified limits during the load flow study, therefore only the equipment loadings require further analysis. All further results outside the verification limits can be seen in Appendix C.

Table 5: Equipment Loading

Overloaded Elements	
Equipment I.D.	**Loading [%]**
TF-04 - 11/0.415kV – 2.5MVA	90.92
TF-11 - 0.415/11kV - 2MVA	88.26
TF-12 - 0.415/11kV - 2MVA	88.2
TF-13 - 0.415/11kV - 2MVA	88.25
TF-14 - 0.415/11kV - 2MVA	88.21
TF-15 - 0.415/11kV - 2MVA	88.26
TF-16 - 0.415/11kV - 2.5MVA	88.61
TF-17 - 0.415/11kV - 2.5MVA	88.58
TF-18 - 0.415/11kV - 2.5MVA	88.63

4.4 Conclusions

The system performs well in regards to maintaining voltage levels during the load flow simulation, with the maximum voltage limit at 1.05pu and the minimum voltage limit at 0.95pu. There were no terminals that exceeded these tolerances during the load flow studies. From Table 16 in Appendix C, it can be seen that upstream of the 11kV switchboard SB001 the voltages are slightly above 1.0pu whereas downstream of SB001 the voltages are below 1.0pu. This is due to the station controller maintaining the voltage at SB001 at 1.0, and in order to do this, the generators operate at voltages higher than their rated 415V. This is in order to overcome the voltage drop between the generator terminals and the 11kV switchboard. Downstream of SB001, the lowest voltage on any of the terminals is 0.952pu at MCC-004. This voltage is low due to the large amount of highly inductive load connected to MCC-004 [27], with DOL and SS motors accounting for 1.94MVA at a power factor of 0.85 lagging. The reactive power draw for these motors is 1.01MVAr, which has a significant impact on the voltage level. This can be illustrated by the simple power system shown in Figure 2, which is a per phase diagram that depicts one phase of a balanced three phase system, where the equation for reactive power can be derived:

Equation 6: Reactive Power

$$Q = \sqrt{\left(\frac{VE}{X}\right)^2 - P^2} - \frac{V^2}{X}$$

This equation for reactive power clearly shows the link between reactive power and voltage, where keeping all other parameters constant and increasing reactive power (Q) will decrease load voltage (V) [28].

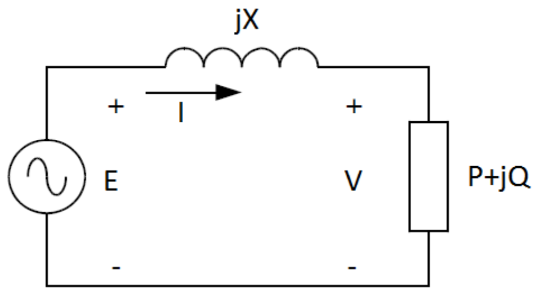

Figure 2: Per-Phase Diagram

This is commonly the case in mine power systems where loads throughout the processing plants are primarily motors that are highly inductive. Referring to Table 16 again, the remaining motor control centre voltages have not been affected as heavily as they are more lightly loaded.

The load flow scenario analysed is for the system operating at maximum demand with 14MW of generation in service and 2MW on standby. The power flows in this situation are well balanced with all generators sharing the load of 13.42MW and 7.41Mvar. The generators operate at 82.12% and 83.19% loading for the 1MW and 1.6MW generators respectively. While the generators operate most efficiently at 68% and 65% loading respectively, the result is acceptable in that the generators are not exceeding rated capacity. The power factor throughout the system is 0.88 lagging, however this is a conservative value due to the assumptions made for loads throughout the system. Modern VSDs will typically operate at close to unity power factor and therefore increase the system power factor however they have been modelled with a power factor of 0.93. The DOL and SS motors will typically operate at power factors higher than 0.85, but for the purposes of the model and simplicity, 0.85 was assumed. Based on all of these assumptions, the load flow study gives a power factor of 0.88, but in practice this would typically be much closer to the Fortescue target of 0.95 lagging.

The results of the load flow study indicate that nine transformers are loaded above the verification threshold of 80% as can be seen in Table 5. Typically this would be cause for concern as most power systems are designed for contingency and future expansion. To allow for this, transformers, cables and other equipment should be loaded less than 80%. In the case of the North Star power system, there will be an additional power station built with its own switchgear and distribution network if Stage Two of North Star goes ahead. Therefore the current loading of equipment is acceptable as there will be no requirement to upgrade or expand upon the current system. Although the step-up transformers TF-11 to TF-18 are loaded above 80%, they are adequately sized to comfortably meet the current proposed load demand. If there are additional load requirements, the loading of the transformers could be reduced by bringing the 2MW of additional generation online, and therefore bringing the additional transformer TF-19 online. This would reduce the current load on each of the step-up transformers to approximately 77% plus any additional load. TF-04 is the transformer that feeds the highly loaded MCC-004, and is loaded at 90.92%. Although MCC-004 has an applied diversity factor of 60%, this could still be an overestimation of the loadings in practice due to the area of the plant operating in two discrete sections. All remaining transformers in the model are lightly loaded and have therefore been sized adequately, as can be seen in Appendix C Table 18 and Table 19.

With reference to Table 17 in Appendix C, the cables in the North Star model all appear to be adequately sized to handle the maximum demand load flow scenario. The most highly loaded cables are those that feed the loads on TF-21 and TF-22 which are loaded at 78%. These loads are large high pressure grinding roll (HPGR) motors. They are modelled as general non-rotating loads for simplicity, as they are fed from variable speed drives. Due to these loads being supplied by VSDs, the loading on the cables will normally be less than 78% for all times when the HPGRs are not running at full capacity.

5 Short-Circuit Analysis

5.1 Background

Short-circuit analysis plays an integral role in the safe operation of power networks and is carried out on all electrical installations. Power systems are designed to supply loads safely and reliably, and while faults in the system will always be possible, they should be minimised and controlled [29].

The purpose of conducting short-circuit studies is to determine the maximum "available" fault current levels at all buses in the system. This allows for the selection of adequately rated protective devices that will be able to interrupt the fault currents without incurring damage. Other electrical equipment such as transformers, cables and busbars must also be rated for the maximum fault currents as they can fail due to thermal and mechanical stresses if subjected to fault currents in excess of their ratings. If thermal capacities are exceeded, the insulation of components can break down due to heat, whereas mechanical stresses can cause vibrations or shaking in equipment that can mechanically destroy components. Thermal heating effects in the system are measured by I^2t where I is the short circuit current magnitude and t is the duration of the short-circuit current. The risk of harm to personnel or the general public is significantly reduced by utilising equipment that is adequately rated to handle the fault currents in the system.

Short-Circuit Effects

The following are some of the effects of short-circuit faults on power systems [29] [7]:

- Arcing and burning at the short-circuit location
- Short-circuit currents flowing from the power sources to the fault location
- Thermal and mechanical stresses on equipment that is subjected to short-circuit currents
- System voltage drops of varying degrees depending on the magnitude of the current
- Loss of synchronism of generating sets
- Major power system blackouts

These effects must be minimised to ensure the safety and reliability of the system. Protective devices such as circuit breakers and fuses must operate quickly to clear the short circuits. In most cases, relays are implemented to control the operation of the circuit breakers. The circuit breakers throughout the system must be accurately coordinated with appropriate discrimination between upstream and downstream breakers. Performing short-circuit studies in software such as PowerFactory allows for a number of different fault scenarios to be analysed in a relatively short time, and allows for coordination of the relays in the system.

Types of Faults

Short-circuit faults can occur in all areas of a power system and occur between phases, between phases and earth, or both. There are several different types of faults including:

- Three-phase (with or without short to earth)
- Single-phase to earth
- Phase to phase
- Two-phase to earth

The three-phase fault is the only balanced short-circuit fault; all other faults are unbalanced and require the use of symmetrical components for analysis. Symmetrical components require the calculation of three independent system components in order to complete the short-circuit calculations. The three components are positive-sequence, negative sequence and zero sequence voltages or currents [18]. Depending on the fault type, different combinations of the sequence components are used to solve for the short-circuit fault current.

The most common type of fault that occurs in industrial power systems is the single-phase to earth fault [7]. Three-phase faults are not as common, however they are the most commonly studied in industry as they usually produce the maximum fault currents that a power system will see. This analysis examines the effects of the maximum and minimum three-phase and single-phase to earth faults.

Causes of faults

There are many different causes of short-circuits including human error, however the majority of faults that occur in power systems are weather related or are caused by equipment failure. A case of human error that causes short-circuit faults is when maintenance workers unintentionally leave isolated equipment connected to earth when reenergizing the system. In order to eliminate this from occurring, there are typically switching procedures that workers must follow. Different weather and environmental factors can cause different types of short-circuits in power systems. The different conditions that can cause faults include lightning, build-up of snow or ice, heavy rain, powerful wind, build-up of salt on insulators and floods or fires [7]. Lightning is the leading cause of short-circuits in overhead line systems where the discharge of current is in the order of a few kilo-amps up to 200kA. The high currents can cause back-flashovers and short-circuits due to the voltage produced across the insulator exceeding the line’s insulation strength. Equipment such as machines, circuit breakers, transformers and cables can fail due to aging insulation, high amounts of switching or lightning over-voltages, mechanical incidents or incorrect installation. An example of equipment failure is a cable’s insulation being cracked due to age, or an excavator cutting into a cable’s insulation, which causes the current to short to ground through the gaps in insulation.

Sources of Short-Circuit Currents

When performing short-circuit calculations all sources of current must be considered. Figure 3 illustrates the four basic sources of short-circuit current that can feed current into a fault such as that shown in the bottom half of Figure 4. In the case of the North Star power system, there are only generators and induction motors present. Generators continue to produce voltage during a short-circuit because the field excitation is maintained and the engine drives the generator at normal speed. The generated voltage produces current of large magnitude that feeds the fault, where the current is only limited by the impedance of the generator and the impedance of the circuit from the generator to the fault location. The impedance of the generator changes with time and as such a complex expression as function of time would be required. For simplification, generator impedance is given in three different reactance values, as seen in the earlier Table 1 for the North Star generators. The first reactance is the subtransient reactance, which is the apparent reactance of the stator winding that the system sees at the time when the short circuit occurs, and determines the magnitude of the current in the first few cycles of the short-circuit event [29]. The second reactance is the transient reactance, which determines the magnitude of the current after the first few cycles up until approximately 500ms, depending on the machine design. The final reactance is the synchronous reactance, which is the reactance the system sees at steady state and determines the steady state current flow. It is unusual for this reactance to be used in short-circuit studies as the fault is typically cleared sooner than the few seconds it takes before this reactance is effective. Induction motors are not as complicated in that they only contribute current to the short-circuit for 2-3 cycles, and only have subtransient reactance. In accordance with AS2067, the contribution of large motors to the short-circuit current are considered.

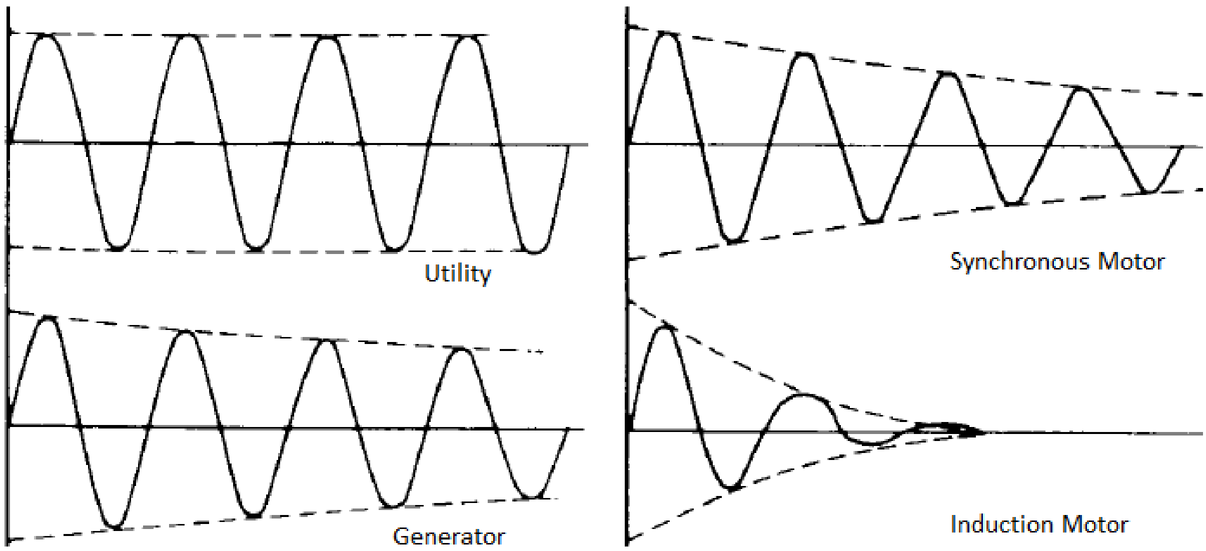

Figure 3: Decreasing Symmetrical Short-Circuit Currents (redrawn from AS3851)

Symmetrical and Asymmetrical Currents

Short-circuit currents are asymmetrical about the zero axis and are analysed in terms of two components - a symmetrical component and an aperiodic component also known as the DC offset. In any short-circuit current there are symmetrical currents that feed into the fault from the sources discussed in the previous section. Typically these components add to give a current similar to that shown in Figure 4 (top half – symmetrical component) where the symmetrical current decays to a steady state due to the apparent change in machine reactance. During the first few cycles after the fault occurs, the current is higher and the magnitude of the current peak is dependent upon when the fault occurs and the decay of the DC component [7]. The maximum peak current generally occurs when the short-circuit starts at the zero crossing of the pre-fault voltage waveform [24]. The DC component of the short-circuit current is introduced to compensate for the current in inductive loads not being able to change instantaneously from its value at the instant the fault occurs to its steady state value [30]. It depends upon the reactance and resistance of the circuit from the point of the fault up to and including the sources. The maximum DC component i_{DC} of the short-current may be calculated with sufficient accuracy by the equation from IEC60909 Section 4.4, which also determines the rate of decay:

Equation 7: DC Current Component

$$i_{DC} = \sqrt{2} I_k'' e^{-2\pi f t \left(\frac{1}{X/R}\right)} \text{ [18]}$$

where

I_k''	is the initial symmetrical short-circuit current (rms);
f	is the nominal frequency;
t	is the time;
X/R	is the ratio of reactance to resistance, note that power factor = $\cos\left(\tan^{-1} X/R\right)$

This shows that the maximum DC component is found at time $t = 0$ giving $i_{DC} = \sqrt{2} I_k''$, which is equal to the amplitude of I_k''. The symmetrical component and the DC component together produce the asymmetrical short-circuit current as can be seen in Figure 4 (bottom half – asymmetrical current).

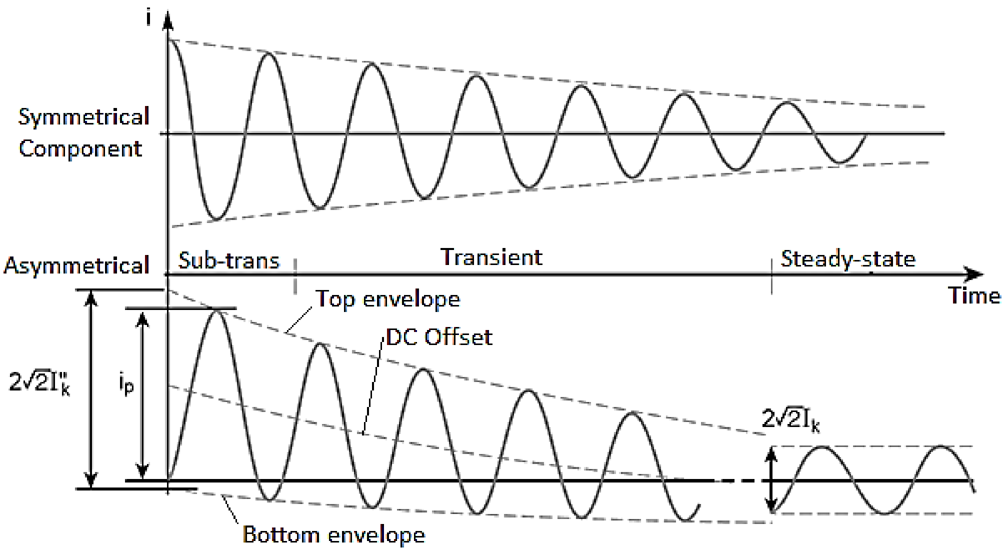

Figure 4: Symmetrical and Asymmetrical Components (redrawn from [29])

5.2 Methodology

Short circuit studies are carried out in PowerFactory using the fault calculation tool, whereby the user selects the method of short-circuit analysis that will be utilised. The most widely used method for calculating short-circuits is the IEC 60909 method, however this method can be overly conservative and does not consider the pre-fault conditions. The primary method that has been used in this analysis is the Complete method, or the Superposition method. The Complete method is more accurate for power systems that are in the stage that the North Star power system is in, where equipment sizes and specifications are known. The Complete method gives more accurate results as the voltages in the network under steady state are considered and "superimposed" onto the results for the short-circuit calculations. In comparison, the IEC60909 method of calculation uses an equivalent voltage source at the faulted location with a voltage "c-factor" applied to give conservatively estimated results. The load currents are neglected in this method and nominal conditions are assumed for the entire network. The IEC60909 method is more applicable to power systems that are in the initial feasibility and design stage, where equipment sizes have not been confirmed; it will be used for comparison in this analysis. The short-circuit studies that are carried out in this report are as follows:

Complete Method:

- Maximum Three-Phase Fault
- Minimum Three-Phase Fault
- Maximum Single-Line to Ground Fault
- Minimum Single-Line to Ground Fault

IEC60909 Method:

- Maximum Three-Phase Fault

The short-circuit faults are carried out on all buses in the system in order to capture all potential fault scenarios that may occur. The maximum short-circuits are calculated with 14MW of generation online and include the contribution of motors. The resistances of the lines are considered at a temperature of 20°C. The maximum short-circuit fault currents determine the rating or capacity of electrical equipment. The minimum short-circuits are calculated with 3MW of generation online and motor contribution is not included. The resistances of the lines are calculated at the maximum end temperature of the conductor using Equation 3 from IEC60909. The minimum short-circuit fault currents can be used as a basis for the selection of protection devices and settings and are useful in determining whether motors will successful start-up without tripping.

The Complete method gives the option of choosing how the system should be initialised at the moment before the short-circuit occurs, whereas IEC60909 automatically implements a voltage c-factor based on the standard. For the Complete method, maximum faults use a load flow for initialisation, whereas for the minimum faults, the initialisation is by voltage c-factor as the load flow does not converge with minimum generation.

The IEC60909 states that voltage c-factor is necessary to account for various effects such as [18]:

- Variations in voltage depending on time and place
- Transformer tap changes
- Omission of loads and capacitances
- Subtransient response of generators and motors

From Table 1 in IEC60909, for the calculation of minimum short-circuits, the c-factor is 0.95 for low-voltage buses and 1.00 for high-voltage buses.

PowerFactory also provides the option of creating plots of the short-circuit currents when using the IEC61363 method of calculation. The three-phase short-circuits are calculated with an equivalent machine that summarizes all active and non-active components on the grid that feeds directly into the short circuit. This method only gives approximate results and has been used to show the short-circuit current response only. The methods and calculations outlined above are those that the short-circuit analysis is centered on.

From IEC60909, there are a number of factors that these calculation methods assume such as:

- All line capacitances shunt admittances of other passive elements are neglected;
- For the duration of the short-circuit calculation, there is no change in the type of fault involved;
- For the duration of the short-circuit calculation, there is no change in the number of circuits involved;

- For the duration of the short-circuit calculation, there is no change in the source voltage.
- Arc resistances are neglected;
- Transformer ratios are taken as the ratio of system nominal voltages, where tap-changers in far-from-generator short-circuits may be disregarded [18].

5.3 Results

The following results were produced with an equipment loading threshold of 80% in order to identify areas of the network that are close to rated capacity. All further results are presented in Appendix D.

The characteristics that are of interest in terms of assessing the loading are as follows:

- The initial rms value of the symmetrical AC component (I_k'')
- The instantaneous peak value of the short-circuit current (I_p)
- The thermal equivalent rms value of the short-circuit current (I_{th})

where I_p and I_{th} are calculated using I_k'' once known.

The busbar and cable loadings are analysed in terms of thermal ratings as given in equipment specifications. The busbars in the model that have specified thermal ratings are the generator busbars (e.g. busbar "TF-16 415V 85kA 1s"), the 11kV switchboard SB001, and the LV MCC buses. The generator busbar "TF-16 415V 85kA 1s" has a thermal rating of 85kA for 1 second, the 11kV switchboard has a thermal rating of 25kA for 1s and the LV MCCs have a thermal rating of 65kA for 1s. Typically, the peak ratings are also analysed in short-circuit studies in order to identify whether the peak short-circuit current is within specified limits. In this case, the peak current is denoted for the purpose of awareness, and the limits are not analysed due to lack of information. It is general industry practise to use a multiplying factor of 2.5 on the thermal rating for the peak rating of equipment. This has been implemented in the results in Appendix D for approximation of the peak loading.

5.3.1 Maximum Three-Phase Fault

Complete

Table 6: Overloaded Busbars Max 3ϕ Complete

Name	Ik"	ip	Ith	Loading, Ith
	kA	kA	kA	%
TF-16 415V 85kA 1s	70.391	167.015	71.290	83.871
TF-17 415V 85kA 1s	70.314	166.679	71.207	83.773
TF-18 415V 85kA 1s	70.386	167.015	71.286	83.865

All further results are given in Table 20 and Table 21 in Appendix D.

IEC60909 Method (for comparison)

Table 7: Overloaded Busbars Max 3ϕ IEC60909

Name	Ik"	ip	Ith	Loading, Ith
	kA	kA	kA	%
TF-16 415V 85kA 1s	73.199	167.910	73.966	87.019
TF-17 415V 85kA 1s	73.118	167.614	73.881	86.919
TF-18 415V 85kA 1s	73.211	167.952	73.979	87.034

All further results are given in Table 22 and Table 23 in Appendix D.

IEC61363 Method

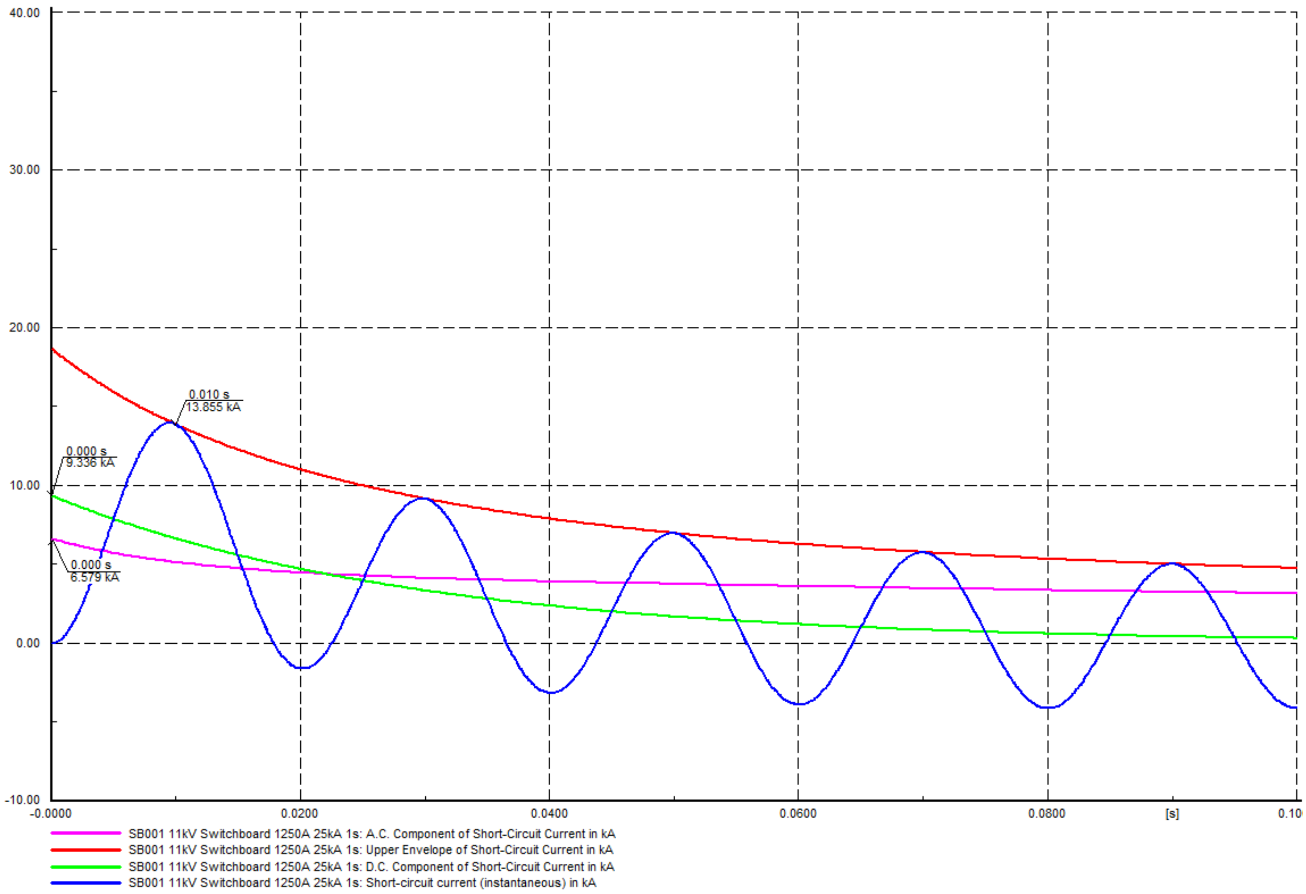

Figure 5: Maximum Three-Phase Short-Circuit (IEC61363)

The IEC61363 method has been implemented for the same maximum three-phase short-circuit scenario in order to illustrate the short-circuit event, however only the results for a short-circuit at SB001 are shown. Figure 5 illustrates the short-circuit current during the first 100 milliseconds of the fault event. The pink curve shows the AC rms component of the symmetrical short-circuit current. The green curve shows the DC component of the short-circuit current which, when combined with the AC component, produces the total short-circuit current. The total asymmetrical short-circuit current waveform is illustrated by the blue curve.

5.3.2 Minimum Three-Phase Fault

There were no elements with loading above the 80% threshold. All results are given in Table 24 and Table 25 in Appendix D.

5.3.3 Maximum Single-Line to Ground Fault

Table 8: Overloaded Busbars Max 1ϕ

Name	Ik" A	ip A	Ithmax	Loading, Ith
	kA	kA	kA	%
MCC-004 ---- 4000A 65kA 1s	53.882	115.600	54.289	83.522
TF-16 415V 85kA 1s	66.411	157.571	67.259	79.128
TF-17 415V 85kA 1s	66.376	157.344	67.219	79.081
TF-18 415V 85kA 1s	66.402	157.562	67.251	79.118

All further results are given in Table 26 and Table 27 in Appendix D.

5.3.4 Minimum Single-Line to Ground Fault

There were no elements with loading above the 80% threshold. All results are given in Table 28 and Table 29 in Appendix D.

5.4 Conclusions

All results given are for the Complete Method of calculation, unless otherwise stated.

5.4.1 Maximum Three-Phase Faults

The maximum three-phase short-circuit fault scenario has highlighted three of 16 possible busbars that are operating close to their thermal loading capacities. Referring to Table 6 in the results section, the busbars on the LV side of the power station transformers TF-16, TF-17 and TF-18 are loaded above the 80% threshold for thermal limits. These busbars are rated for 85kA for 1s, and are all loaded at just under 84% with equivalent thermal current of approximately 71kA. These busbars are highly loaded compared to the six other power station transformer LV busbars. This is due to these busbars having two active 1MW generators connected to each bus, whereas the remaining busbars have one 1.6MW generator connected, or two inactive 1MW generators. At 84% loading, there is still capacity for thermal current to flow in these busbars and this does not pose a significant concern for the power system.

IEC60909

The IEC60909 method has identified the same three busbars as being loaded above the 80% thermal capacity threshold as given in Table 7. Compared to the Complete method results of 84% loading, the busbars are loaded at approximately 87% which illustrates the more conservative calculation techniques of IEC60909. As these results are approaching 90% it could pose a concern for the power system if the components are frequently subjected to maximum short-circuit currents or other events such as sustained over-voltages [31], however this is an unlikely problem. The busbars are unlikely to be exposed to maximum fault currents of this magnitude as the results are conservative in nature and the Complete method results are more accurate due to using pre-fault conditions in the calculation.

5.4.2 Minimum Three-Phase Fault

The minimum three-phase short-circuit scenario did not cause any elements to be loaded above the 80% thermal capacity threshold. These results are discussed in detail in the following section.

5.4.3 Maximum Single-Line to Ground Fault

The maximum single-line to ground short-circuit fault scenario has highlighted just one busbar that is loaded above the 80% thermal capacity threshold shown in Table 8. Interestingly, MCC-004 is loaded at 83.5% during this fault scenario compared with 71% in the three-phase fault scenario. While 83.5% loading is not a significant cause for concern, the increase compared to the three-phase fault scenario does pose some questions. In both cases, the initial symmetrical fault current (I_k'') is approximately 54kA, whereas the thermal current (I_{th}) over 1 second increases from 46kA in the three-phase fault to 54kA in the single-phase fault. Typically, when zero-sequence impedances are significantly lower than the positive sequence impedance, the fault current increases during single-phase faults; although in this case I_k'' is very similar and it is I_{th} that is changing. This indicates that the subtransient impedances are the same, and the transient impedance is lower in the single-line to ground fault than in the three-phase fault. The PowerFactory calculation method for the thermal current is over the time of one second, therefore the single-line to ground short-circuit current must decay more slowly than the three-phase fault and therefore the single-phase thermal short-circuit current is higher for that period of time.

5.4.4 Minimum Single-Line to Ground Fault

The minimum single-line to ground short-circuit scenario did not cause any elements to be loaded above the 80% thermal capacity threshold. These results are discussed in detail in the following section.

5.5 Protection Coordination

5.5.1 Background

The verification of protection settings for the North Star power system has been carried out for all HV protection relays in PowerFactory. The recommended protection settings as given in Appendix D were supplied to Fortescue by the contracted external consulting agency, Petro Min Engineers, who are subcontracted via the main contractor for North Star, UON Pty Ltd. The internship timeline did not coincide directly with the North Star project timeline and therefore the majority of the design works were carried out before the internship began. As a result, the internship did not cover the design and recommendation of protection settings, rather the verification of the recommended protection settings in the PowerFactory model. The minimum fault levels are used to assess the protection setting coordination, where the minimum number of generators online is 3x 1MW generators. For the purposes of this analysis, the Generators that are online are GN-09, GN-10, and GN-11 and therefore the transformers online are TF-17 and TF-18.

A summary of the protection functions that are used in each relay is given in Table 9. The protection functions in bold have been replicated in the PowerFactory model. All remaining functions could not be replicated due to the function not being available in the relay type in PowerFactory, or the relay type not being available at all. The "Masterpact NW40H2 Micrologic 5.0E" does not exist in the PowerFactory library, however the Schweizer "SEL751A" relay is available. Therefore this analysis does not cover the protection and coordination with the Generator Circuit Breakers (GCBs) and coordination is assessed with the Generator Transformer Circuit Breakers (GTCBs) only. The reverse power function in the GTCBs is provided to isolate the upstream fault. The GCBs are set to disrupt the fault if the neutral current still exists after the relay trips the GTCBs.

The protection settings for each of the protection functions in Table 9 are given in Appendix D: Protection Settings. These settings are taken directly from one of Fortescue's internal documents. Using these protection settings in the PowerFactory model, the time-overcurrent curves were plotted and assessed for correct grading, where one of each example is analysed below.

Table 9: Protection Functions

No.	Equipment	Relay Type	Protection Function
1	415V 1MW Generator Circuit Breaker (GCB)	Masterpact NW40H2 Micrologic 5.0E	50P/51P: Phase Overcurrent
2	415V 1.6MW Generator Circuit Breaker (GCB)	Masterpact NW40H2 Micrologic 5.0E	50P/51P: Phase Overcurrent
3	415V 2.5MVA Generator Transformer Circuit Breaker (GTCB)	Masterpact NW40H2 Micrologic 5.0E and SEL-751A	**50P/51P: Phase Overcurrent** **50N: Neutral Overcurrent** 32P: Reverse Power 50Q: Negative Sequence Overcurrent Arc Flash Protection
4	415V 2MVA Generator Transformer Circuit Breaker (GTCB)	Masterpact NW40H2 Micrologic 5.0E and SEL-751A	**50P/51P: Phase Overcurrent** **50N: Neutral Overcurrent** 32P: Reverse Power 50Q: Negative Sequence Overcurrent Arc Flash Protection
5	11kV 3.554MVA HPGR Drive Feeders	SEL-751A	**50P/51P: Phase Overcurrent** **50G: Ground Overcurrent**
6	11kV 2.5MVA Transformer Feeders	SEL-751A	**50P/51P: Phase Overcurrent** **50G: Ground Overcurrent**
7	11kV Earthing Transformer Feeder	SEL-751A	**50P/51P: Phase Overcurrent** **50N: Neutral Overcurrent**
8	11kV Auxiliary Transformer Feeder	SEL-751A	**50P/51P: Phase Overcurrent** **50G: Ground Overcurrent**

5.5.2 Results and Conclusions

It was found that normal operating currents do not trip any of the relays, which indicated correct pick-up current settings. All short-circuit currents stated within Section 5.5.2 are referred to the HV side.

5.5.2.1 2.5MVA Step-Down Transformer Feeders and GTCBs

The 2.5MVA step-down transformer feeders and the GTCBs must grade adequately in order to avoid loss of power to the system where it is not necessary. For the purposes of this analysis, only one fault is carried out at MCC-003 and the TF-03 feeder is analysed for coordination with the TF-17 and TF-18 feeders. This is possible as the short-circuits at the other MCCs are of similar magnitude as can be seen in Table 24 in Appendix D, and as such will behave in a very similar manner. Figure 6 illustrates the scenario where a minimum three-phase short-circuit fault occurs at MCC-003, therefore the relay protection curve for the circuit breaker (CB) protecting the TF-03 feeder has been plotted with the online transformer GTCBs. The minimum fault is studied in order to determine whether the correct relay will trip within the desired timeframe. From Figure 6 it appears that the protection settings for the TF-03 feeder CB are adequately designed as this relay will trip the short-circuit current of 563.5A in 0.646s. If this relay/circuit breaker were to fail, the coordination with the GTCBs upstream is such that they will not trip until 1.412s and 2.742s following the short-circuit event for the TF-18 feeder and TF-17 feeder respectively. The reason the tripping times are different for the TF-18 and TF-17 feeders is due to more current flowing through TF-18 as it is supplied by two online 1MW transformers whereas TF-17 is supplied by one. This is an acceptable margin of discrimination as it leaves little room for error.

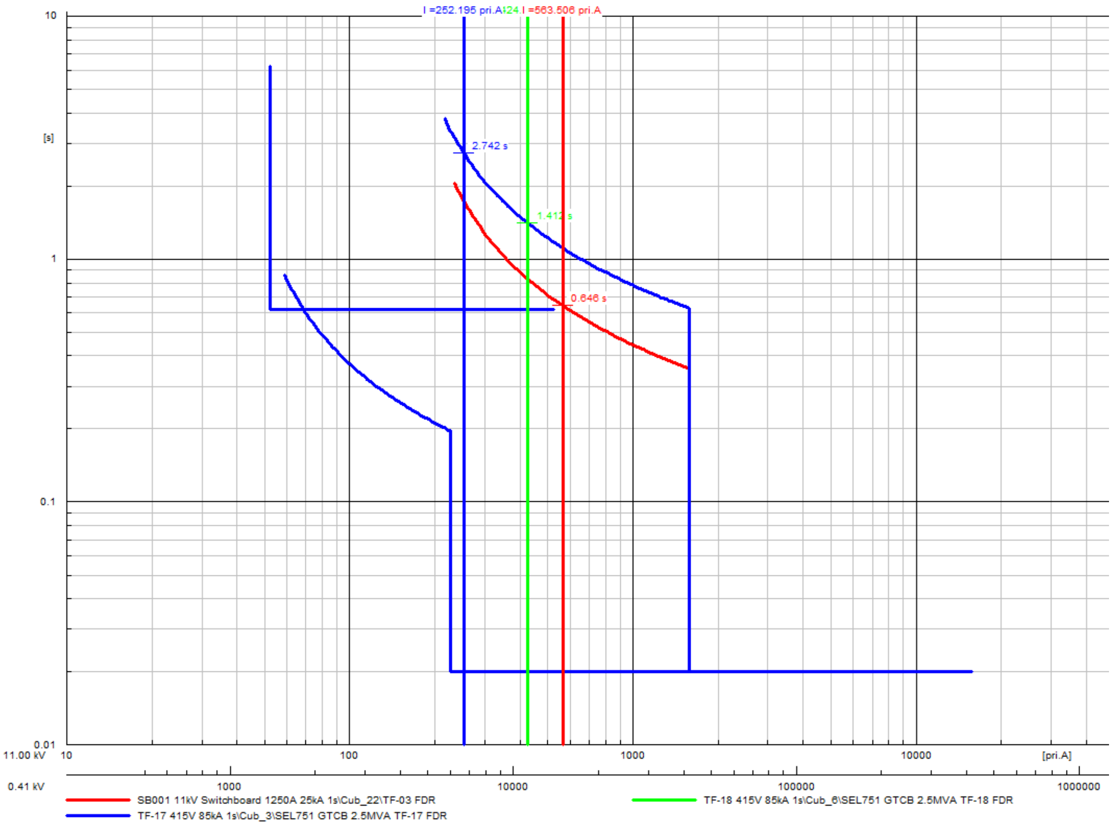

Figure 6: 2.5MVA Step-Down Transformer Feeders and GTCBs

When carrying out protection studies, it is also recommended to assess the start-up of the largest DOL motor so that it can successfully start without causing the circuit breaker to trip on overcurrent. The largest DOL motor throughout the entire system is connected via MCC-003. Only this motor is required to be assessed against protection settings as all other smaller DOL motors have inrush curves less than the largest DOL motor. It is also good practice to analyse the large VSDs and SSs as these motors can have similar effects if they are significantly larger than the DOL motor. For the purposes of this analysis, only the largest DOL motor has been assessed for coordination in order to give an example. The next chapter will cover motor starting in depth, and take into account VSDs and SSs as well as DOL motors.

In this model, only the HV circuit breakers are considered for the feeders and therefore only the relay feeding TF-03 is plotted. However in a power system, there is typically another relay and circuit breaker/air circuit breaker/moulded case circuit breaker on the MCC incomer. The MCC incomer protects the MCC and all loads connected to the MCC and will therefore have tighter protection settings than the feeder relay. Figure 12 illustrates a typical 150kW motor starting curve from the PowerFactory library (green curve) and the TF-03 feeder relay curve (blue curve). The motor can start successfully without causing the relay to operate on overcurrent due to the high inrush current of the motor, therefore the relay is graded adequately for motor starting.

5.5.2.2 3.554MVA HPGR Drive Feeders and GTCBs

The HPGR Drive Feeders and GTCBs must have a sufficient degree of discrimination in order for the HPGR Drive Feeders to trip before the GTCBs in short-circuit conditions. A minimum three-phase short circuit was performed on the 1.903kV side of TF-21 which produced a prospective short-circuit current of 519A on the 11kV side and through the HPGR Drive Feeder Relay as shown in Figure 13. In comparison, the TF-18 and TF-17 feeder relays will not trip until 1.474s and 2.983s respectively, indicating a sufficient degree of discrimination.

5.5.2.3 Auxiliary Transformer Feeder and GTCBs

The 500kVA Auxiliary Transformer Feeder relay must grade adequately with the GTCBs in order to trip before the GTCBs. Figure 14 illustrates the time-overcurrent curves for these relays and shows that a fault at DB101 on the LV side of TF-01 produces a short-circuit current of 300.6A that is interrupted at 0.423s. In comparison, the TF-18 and TF-17 feeder relays trip at 1.852s and approximately 5s respectively.

5.5.2.4 Earthing Transformer Feeder and GTCBs

The discrimination between the Earthing Transformer Feeder relay and the GTCBs must also be sufficient for the phase overcurrent curves. Figure 15 illustrates the protection relay curves where a fault on the node between the earthing transformer feeder cable and the transformer produces a short-circuit current of 1.09kA and trips instantaneously. Conversely, the tripping times for TF-18 and TF-17 are 0.974s and 1.47s respectively.

5.5.2.5 2.5MVA Step-Down Transformer Feeders and Earthing Transformer CB

The earth fault settings are also assessed for coordination. Figure 16 illustrates the HV earth overcurrent settings of the earthing transformer feeder and the TF-05 feeder. All of the 2.5MVA step-down transformer feeders have the same settings, and therefore the TF-05 feeder is used for this example. Performing a minimum single line to ground fault on the 11kV board, or any other HV busbar produces a short-circuit current of 73.3A. If the fault is on the 11kV side of TF-05, the TF-05 feeder relay will trip this short-circuit at 0.320s and the earthing transformer feeder will trip at 0.720s indicating an adequate coordination delay. The maximum earth current is limited by the earthing transformer to 100A (the calculation gives 99.8A) and will have the same tripping times as shown in the figure.

6 Motor Starting Studies

6.1 Background

Motor starting studies are important indicators of how a power system will respond to certain operating scenarios. When motors are started they draw a large inrush current typically 3 to 7 times the full load current of the motor. This is due to the large amount of energy required to magnetise the motor enough to overcome being at standstill [32]. As a result of the high transient starting currents, the voltage drops at the motor terminals and throughout the system. The high starting currents also cause equipment in the system to experience higher loading than under normal operation.

There are various ways to reduce the starting current of motors by connecting the motors through a type of soft starter (SS) or variable speed drive (VSD), depending on the motor's application. Larger motors are typically connected to the system through a SS or VSD, while smaller motors are connected by a direct-on-line starter. In order to assess whether the system is adequately designed, motor starting studies have been carried out on the largest motors to analyse the resulting voltages in the system and the loading of transformers. This analysis includes the largest DOL motor on each MCC, the largest SS connected motor and the largest VSD connected motor out of all the MCCs.

The starting of large motors causes the voltage at the motor terminals to drop and also causes fluctuations in the voltages upstream. The electrical installation should be designed such that it can withstand the effects of motor start-ups, but if the system is inadequately designed, the voltage drop can cause problems such as:

- Unnecessary operation of relays on under-voltage trips
- Overloading of electrical equipment
- Flickering lights throughout the system
- Failure to start the motor due to low starting torque [33]
- Stalling of other connected motors [26]

To prevent problems like this from occurring, the voltage should not be permitted to drop below 80% of the nominal rating [26]. While 80% is a typical threshold used in industry, the Fortescue Specification 100-SP-EL-0001 states that the maximum voltage drop at the motor terminals is 15%, therefore the voltage cannot drop below 85% of the nominal voltage for the North Star model.

6.2 Methodology

In order to analyse the performance of the system during motor starting, each motor was simulated from start-up for 5 seconds. When running motor starting studies, PowerFactory computes a load flow study initially to determine the operating currents throughout the rest of the system, after which the selected motor is started. The motor current, active power, reactive power and speed values were then plotted against time. This is a built in function of PowerFactory to provide these outputs upon running a motor starting study, where the simulation time is the user's preference. Following this, the voltage at the relevant MCC was plotted against time to illustrate the point at which the MCC voltage reached the lowest point. The time at which the MCC voltage was a minimum was then used as the simulation time for another motor starting study on the same motor. The reason for doing this is to stop the simulation at the point in time when the voltage has dipped to the lowest value, and show the effect on the rest of the system voltages. This gives the worst case scenario in terms of motor starting, and the loading of the relevant transformer can also be seen. The analysis does not cover the loading of cables as the cables downstream of the 11kV switchboard are largely oversized and the loading does not surpass 50% in the worst case scenarios.

6.3 Results

The system has been analysed in three different states for comparison:

- During start (lowest voltage point)
- During start (after 5 seconds)
- Normal operation (steady state)

Under each scenario, the voltages at the motor terminals have been captured as well as the other bus voltages throughout the system from the 11kV switchboard and downstream. The motor that has the greatest impact is the largest DOL motor on the system, the 150kW motor on MCC-003. The results of this scenario are illustrated in Table 10 and the summary of the transformer loading during motor starting is shown in Table 11. All other results for the different motor starting scenarios can be seen in Appendix E, from Table 30 to Table 35. The motor starting characteristics for the DOL motors are given in Figure 17 to Figure 21.

Table 10: MCC-003 150kW DOL Motor Start-Up

Bus Voltages (p.u.)			
Bus I.D.	**During Start (0.663s)**	**During Start (5s)**	**Normal Operation**
SB001	0.92	0.93	1.0
DB101	0.91	0.93	0.993
MCC-002	0.89	0.9	0.965
MCC-003	**0.85**	**0.9**	**0.965**
MCC-004	0.88	0.89	0.952
MCC-005	0.9	0.91	0.974
MCC-007	0.89	0.91	0.969

Table 11: Transformer Loading During DOL Motor Start-Up

Transformer Loading (%)			
	During Start (Lowest Voltage Point)	**During Start (After 5s)**	**Normal Operation**
TF-02	92.35	71.95	79.11
TF-03	113.66	68.94	70.79
TF-04	106.26	92.83	90.92
TF-05	68.38	53.91	55.74
TF-07	90.53	63.74	65.53

6.4 Conclusions

During start-up of the 150kW motor on MCC-003, the voltage reaches the lowest point of 0.85pu at 0.663s. This is the lowest voltage that the system experiences during any of the motor starting scenarios, and is on the threshold of compliance with the Fortescue Specification which states that the transient voltage drop shall be a maximum of 15%. After 5 seconds when the motor has reached nominal speed and current, the voltage at MCC-003 is just 0.9pu compared to steady state when the voltage is 0.965pu. This demonstrates that motors cause the system to experience voltage sags, however the system does recover which is the important outcome. As can be seen from Table 10, the start-up of the 150kW motor on MCC-003 has a flow on effect on the voltages throughout the system. This is important because if the effect is too great then flickering of lights may be experienced and stalling of other connected motors may occur. The other system voltages do not sag lower than the threshold of 0.85pu and therefore these effects are unlikely to be experienced.

In the case where the 150kW motor on MCC-003 is started, the transformer TF-03 that feeds MCC-003 experiences loading of 113.66% due to the inrush current, as can be seen in Table 11. This is the scenario that causes the highest loading of any transformer throughout the model. After 5s, the transformer is not yet loaded up to what it is at normal operation due to the voltage not yet recovering entirely. As can be seen from the table, the transformer is typically loaded at 70.79%, which is significantly lower than rated capacity. It is for this reason that the transformer is permitted to be loaded higher than 100% for short periods of time, as long as it is balanced by periods of under loading. The method for calculating the permissible loading can be found in IEC (or AS) 60076-7. However these standards and methods are typically for transformers that will be overloaded for extended periods of time [34]. In cases where the transformer experiences overloading due to transients the temperature of the transformer is unlikely to climb to significantly high levels. Therefore it will not have a detrimental effect on the transformer windings, oil and insulation as can typically occur in constantly overloaded transformers [35]. The remaining transformers do not experience such high loading as the motors are smaller and therefore the inrush currents are lower.

There are two other scenarios that have been examined for system reliability. Motors that are connected through variable speed drives and soft starters can have an impact on the system if the motors are large enough. Table 34 and Table 35 in Appendix E show the results of starting the 600kW VSD on MCC-002, and the 355kW SS on MCC-007. Under normal operation, the 600kW motor draws rated power and current and the voltage at MCC-002 is 0.965pu with the transformer TF-02 loaded at 79.11%. However during start-up of this motor, the VSD can draw 1.5 times full load current [36], causing the transformer to be loaded at 93.04% and the voltage at the MCC to drop to 0.959pu. Similarly, soft-starter connected motors can have a significant impact on the system if they are large enough. Soft-starters limit the inrush current to 3 times full load current [37], and in this case starting the 355kW motor on MCC-007 causes the transformer to be loaded up to 94.54% from the normal loading of 65.53%. It is important to analyse these scenarios to be aware of the situations that the power system is exposed to, and to be sure that the system can withstand these start-up transients.

7 Conclusion

Modelling the North Star Stage One power system allowed several different operating scenarios to be analysed. The safety and reliability of the system was assessed by determining the current flows in different operating conditions and analysing the effects on system equipment.

Performing load flow analyses illustrated the loading of equipment and stability of the system under steady-state operation. The load flow scenario carried out was the normal proposed operation of the system at maximum demand. The load flow study indicated that all busbars in the system remained within the normal voltage limits of ± 5% and no equipment was loaded above rated capacity. This is a positive outcome for the system reliability and safety as there is minimal risk of damage or harm due to overloading of equipment.

The purpose of conducting the short-circuit studies was to determine whether equipment could withstand the prospective fault currents in the system, and therefore remain within their thermal and mechanical limits. The short-circuit studies that were performed were for the maximum and minimum three-phase and single-line to ground faults at all buses in the system. While the maximum short-circuits caused some busbars to become loaded above 80% of the thermal limits, there were not any major causes for concern. As the thermal and mechanical limits were not exceeded, this indicates that the system will perform reliably and safely under fault conditions.

The coordination of protective devices is paramount in the safety of power systems and was verified for the North Star power system. In all cases where grading was necessary, the delays between levels of protection were acceptable and would not be likely to cause any nuisance tripping.

Motor starting studies were carried out in order to determine the transient response of the system due to the large inrush currents that the motors required to successfully start. The motor starting studies were performed on the largest direct-on-line motor on each low voltage MCC, and the largest variable speed drive and soft starter driven motors on any of the MCCs. The results indicated that the system performs well in regards to motor starting, where no busbars exceeded the maximum allowed voltage drop of 15% during transient conditions.

As a result of the various studies undertaken on the North Star power system, there is now supporting evidence that the system will perform safely and reliably in practice.

8 Future Work

There are a number of areas within the North Star power system model that could potentially be improved by carrying out additional work in the future. Internship placements in industry often illustrate one component of a larger project being completed, and as such, there are usually areas that can be developed further.

For the North Star power system model, this could be improved in the near future by taking measured load information once the system is in operation. This would increase the accuracy of the model to a degree that would otherwise be very difficult to achieve.

As the model is for the North Star Stage One development, the model could be further improved when Stage Two begins. Although Stage Two will have additional generation, distribution and switchgear, there will likely be a point where the systems will combine with a normally open bus tie. This has been implemented in other site power systems in the past.

For the protection coordination, the protection settings were only verified for the SEL-751A relays that were available in the PowerFactory library. This could be extended by adding the relay type for the additional relays on site, such as the MasterPact NW40H2 relays.

Arc-flash studies can be carried out in the later versions of PowerFactory. When Fortescue upgrades to the latest version, arc-flash studies will be carried out on the models that Fortescue maintains. The North Star model would be a good system to start with.

The modelling and analysis of other Fortescue power systems could be carried out, whereby protection settings can be added and integrated into the online database StationWare. This project is already underway at Fortescue, and will inevitably include the North Star model in the future.

Bibliography

[1] Fortescue Metals Group Ltd, “Quarterly Report,” 30 September 2014. [Online]. Available: http://www.fmgl.com.au/UserDir/AsxAnnouncement/Fortescue%20Quarterly%20Report%20September%202014795.pdf. [Accessed 05 October 2014].

[2] Fortescue Metals Group, “Fortescue Executes US$1.5bn Joint Venture Agreement with Formosa,” 16 08 2013. [Online]. Available: http://fmgl.com.au/UserDir/AsxAnnouncement/1246243724.pdf. [Accessed 29 08 2014].

[3] EnergySafety, “WA Electrical Requirements,” January 2014. [Online]. Available: http://www.commerce.wa.gov.au/sites/default/files/atoms/files/waer_2014_0.pdf. [Accessed 09 September 2014].

[4] Fortescue Metals Group, “Standard Engineering Specification for Electrical Design Criteria,” Perth, 2011.

[5] UON Pty Ltd, “Generator Data Sheet PP1250,” UON Pty Ltd, Malaga, 2014.

[6] UON Pty Ltd, “Generator Data Sheet PP2000,” UON Pty Ltd, Malaga, 2014.

[7] N. D. Tleis, “Power Systems Modelling and Fault Analysis: Theory and Practice,” Burlington, 2008.

[8] B. Bridger, “X/R Ratio,” Houston, 1993.

[9] DIgSILENT GmbH, “Two-Winding Transformer (3-Phase),” Gomaringen, 2010.

[10] UON Pty Ltd, “Transformer Data Sheet 2.0MVA,” UON Pty Ltd, Malaga, 2014.

[11] UON Pty Ltd, “Transformer Data Sheet 2.5MVA,” UON Pty Ltd, Malaga, 2014.

[12] UON Pty Ltd, “Transformer Data Sheet 500kVA,” UON Pty Ltd, Malaga, 2014.

[13] Timestar Holdings Pty Ltd, “Transformer 2000/2500kVA - Specification,” Timestar Holdings Pty Ltd, Madeley, 2014.

[14] UON Pty Ltd, “Earthing Transformer Data Sheet,” UON Pty Ltd, Malaga, 2014.

[15] Fortescue Metals Group Ltd, “Transformer 2400kVA 11CST/2.2kV,” Fortescue Metals Group Ltd, East Perth, 2014.

[16] Weir Minerals Australia Ltd, “Transformer Data Sheet 3554/1777/1777,” Weir Minerals Australia Ltd, Artarmon, 2014.

[17] B. L. Capehart, “Equipment Load Factors, Use Factors and Diversity Factors As Well as a General Discussion of Energy Audit Procedures,” 2000. [Online]. Available: www.ise.ufl.edu/capehart/diversity.doc. [Accessed 02 10 2014].

[18] International Electrotechnical Commission, “IEC 60909-0:2001 - Short-circuit currents in three-phase a.c. systems - Part 0: Calculation of Currents,” International Electrotechnical Commission, Geneva, 2001.

[19] WorleyParsons, “FMG Wet Front End Project: Power System Study Report,” WorleyParsons, Perth, 2011.

[20] DIgSILENT GmbH, “Power Factory 14.1 User's Manual,” DIgSILENT GmbH, Gomaringen, 2011.

[21] ABB (a), “Low Voltage: Process performance motors according to Australian MEPS,” May 2014. [Online]. Available: http://www05.abb.com/global/scot/scot234.nsf/veritydisplay/475bc8a9f34daf87c1257cdd001a16c9/$file/Catalog%20for%20Process%20performance%20motors%20acc%20to%20AU%20MEPS_05-2014_LOW.pdf. [Accessed 07 10 2014].

[22] ABB (b), “Low Voltage Motors: Motor Guide,” February 2014. [Online]. Available: http://www05.abb.com/global/scot/scot234.nsf/veritydisplay/a7c16f0e10f4a826c1257c9000270ce0/$file/MotorGuide_february2014_low_FINAL%20with%20bookmarks.pdf. [Accessed 07 10 2014].

[23] Fortescue Metals Group Ltd. Engineering, “Standard Engineering Specification: Low Voltage Induction Motors,” Perth, 2013.

[24] Australian Standards, “AS3851-1991: The calculation of short-circuit currents in three-phase a.c. systems,” Standards Australia, Homebush, 1991.

[25] ABB (d), “ABB Industrial Drives Catalog: ACS800, single drives, 0.75 to 6000 hp,” 15 August 2009. [Online]. Available: http://www05.abb.com/global/scot/scot239.nsf/veritydisplay/411ac81f6a476367852574630063b4d2/$file/acs800-phtc01u-en.pdf. [Accessed 30 October 2014].

[26] C. Bayliss and B. Hardy, Transmission and Distribution Electrical Engineering, Oxford: Newnes, 2007.

[27] B. A. Ellis, “Capacitors,” 01 January 2008. [Online]. Available: http://www.jethroproject.com/Capacitors.pdf. [Accessed 01 November 2014].

[28] G. Crebbin, “Murdoch University ENG455 Lesson 1: Power Systems Protection and Control,” Murdoch, 2014.

[29] GE, “Electrical Distribution and Control - Short-Circuit Current Calculations: For Industrial and Commercial Power Systems,” Plainville, 1989.

[30] D. Sweeting, “Applying IEC 60909, Fault Current Calculations,” *IEEE Transations on Industry Applications,* vol. 48, no. 2, pp. 575-580, 2012.

[31] Novaris, “Main Swichboard and Distribution Board Surge Protection,” Novaris, 2004. [Online]. Available: http://www.novaris.com.au/images/stories/Sales%20Kit/SK05/SF3200.pdf. [Accessed 17 November 2014].

[32] ABB (c), “Technical Note: Starting Methods for AC Motors,” 2010. [Online]. Available: http://www04.abb.com/global/seitp/seitp202.nsf/e308f3e92d9a8fc5c1257c9f00349c99/20a5783a8b31d05748257c140019cc05/$FILE/Technical+note+TM008+low.pdf. [Accessed 29 October 2014].

[33] PowerApps, “Motor Starting Studies,” August 2008. [Online]. Available: http://www.powerapps.org/PAES_MotorStartingStudies.aspx. [Accessed 29 October 2014].

[34] Standards Australia, “AS.NZS 60076.1:2014 Power Transformers - Part 1: General,” Standards Australia, Sydney, 2014.

[35] Standards Australia, “AS/NZS 60076.7:2013 Power Transformers - Part 7: Loading Guide for Oil-Immersed Power Transformers,” Standards Australia, Sydney, 2013.

[36] ComEd, “Variable Speed Drives: Fact Sheet,” 2012. [Online]. Available: https://www.comed.com/Documents/business-savings/fact-sheets/VSD_FS.pdf. [Accessed 12 November 2014].

[37] ABB (e), “Softstarter Handbook,” November 2010. [Online]. Available: http://www05.abb.com/global/scot/scot209.nsf/veritydisplay/6b4e1a3530814df0c12579bb0030e58b/$file/1sfc132060m0201.pdf. [Accessed 12 November 2014].

[38] Fortescue Metals Group Limited, “North Star Project Stage 1: Sitewide Power Distribution SLD,” Fortescue Metals Group Limited, East Perth, 2014.

[39] UON Pty Ltd, “Protection Settings - Document Title: 661MIC0010-5610-RP-EL-0005,” UON Pty Ltd, Malaga, 2014.

Appendix A: North Star

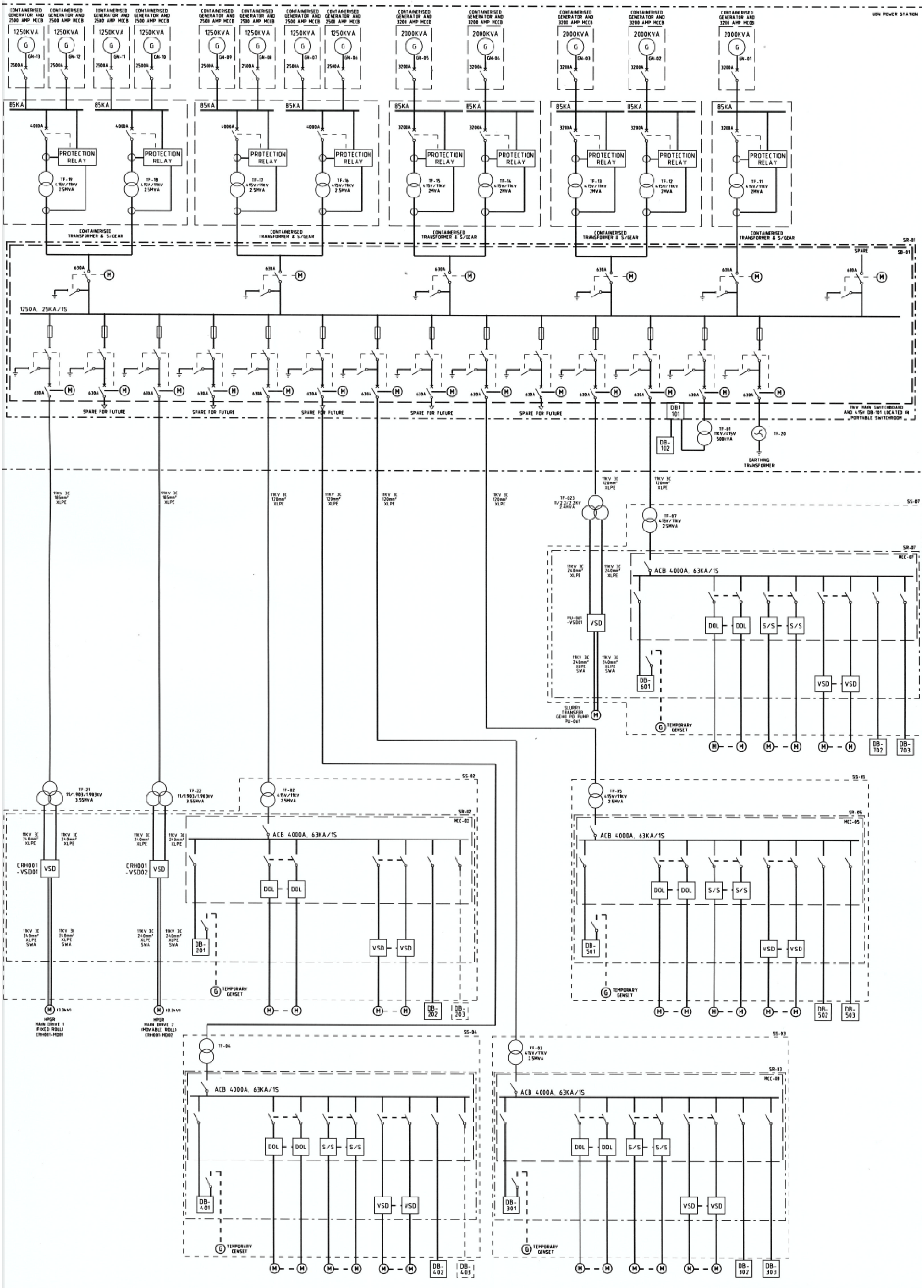

Figure 7: North Star Single Line Drawing [38]

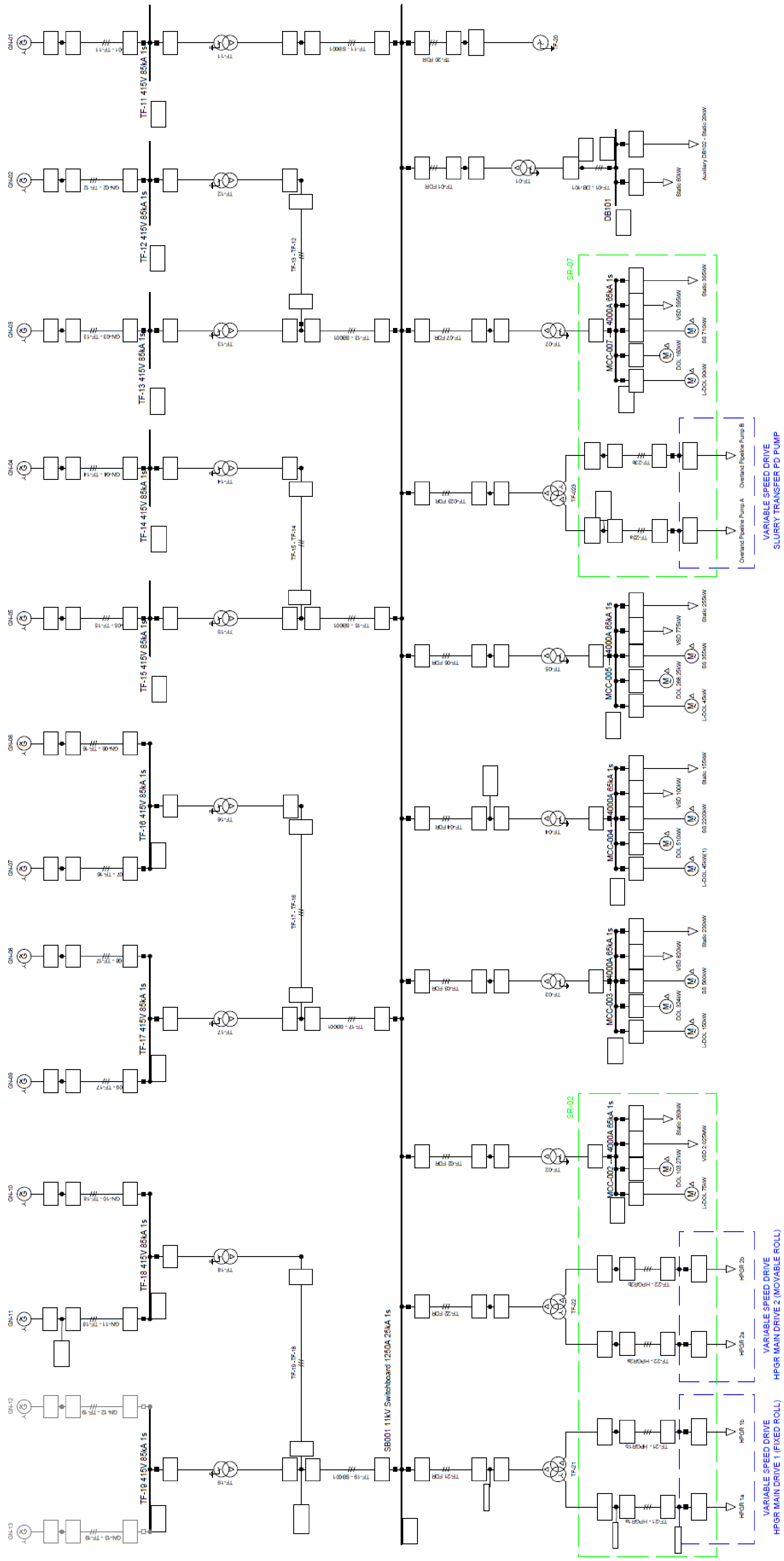

Figure 8: North Star PowerFactory Model

Appendix B: PowerFactory Input Data

Generator Efficiency Curves

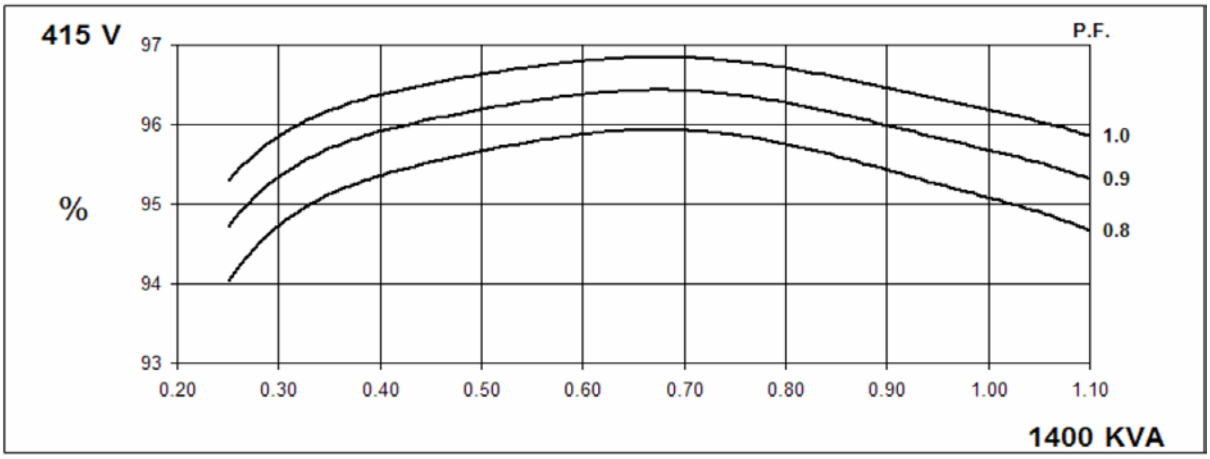

Figure 9: 1400kVA Generator Efficiency Curve [5]

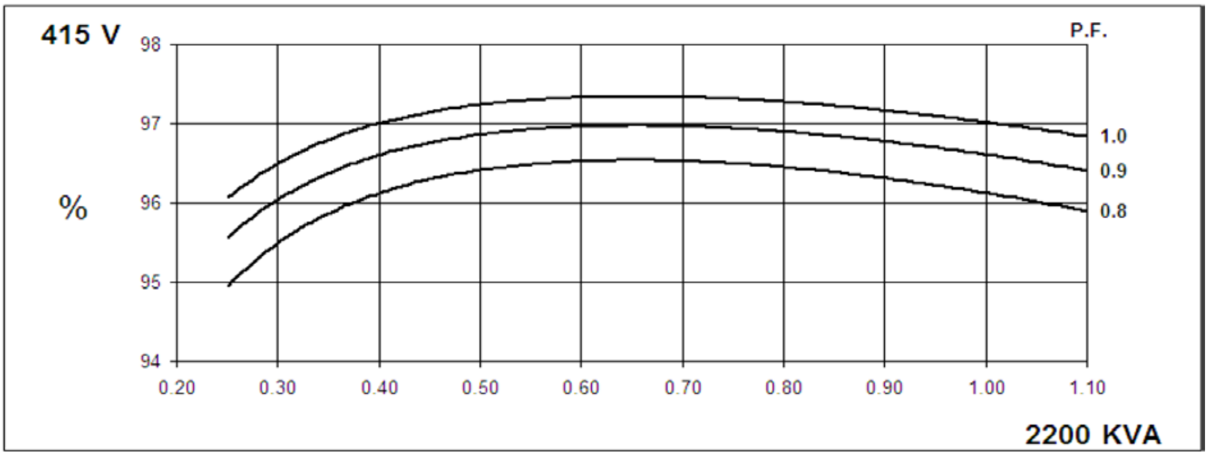

Figure 10: 2200kVA Generator Efficiency Curve [6]

Cable Information

Table 12: Conductor Types

Type	Rated Voltage	Rated Current	Rated SC Current	Nominal Freq.	Phases	No. of Neutrals	R' (20°C)	X'
	kV	kA	kA (1s)	Hz			Ohm/km	Ohm/km
120mm2 6.35-11kV 3C Cu XLPE Screened PVC	11	0.32	17.2	50	3	0	0.154	0.1
150mm2 3x1c Cu XLPE 6.35 11kV	11	0.395	21.45	50	3	0	0.12547	0.114
185mm2 6.35-11kV 3C Cu XLPE Screened PVC	11	0.405	26.5	50	3	0	0.101	0.0942
240mm2 6.35-11kV 3C Cu XLPE Screen HPGR	1.903	0.445	34.3	50	3	0	0.0784	0.0875
240mm2 6.35-11kV 3C Cu XLPE Screened PVC	2.2	0.445	34.3	50	3	0	0.0784	0.0875
300mm2 0.6-1kV 2x1C Cu XLPE PVC	0.415	1.46	79.2	50	3	1	0.1019	0.1263
300mm2 0.6-1kV 3x1C Cu R E 110 PVC	0.415	2.19	118.8	50	3	1	0.0679	0.0842
300mm2 0.6-1kV 5x1C Cu R E 110 PVC	0.415	3.65	198	50	3	1	0.0408	0.0505

Table 13: Cable Locations and Lengths

Name	Type	Terminal i	Terminal j	Length
				km
GN-01 - TF-11	300mm2 5x1C Cu R E 110 PVC	G1	TF-11	0.014
GN-02 - TF-12	300mm2 5x1C Cu R E 110 PVC	G2	TF-12	0.017
GN-03 - TF-13	300mm2 5x1C Cu R E 110 PVC	G3	TF-13	0.014
GN-04 - TF-14	300mm2 5x1C Cu R E 110 PVC	G4	TF-14	0.017
GN-05 - TF-15	300mm2 5x1C Cu R E 110 PVC	G5	TF-15	0.014
GN-06 - TF-16	300mm2 3x1C Cu R E 110 PVC	G6	TF-16	0.016
GN-07 - TF-16	300mm2 3x1C Cu R E 110 PVC	G7	TF-16	0.012
GN-08 - TF-17	300mm2 3x1C Cu R E 110 PVC	G8	TF-17	0.014
GN-09 - TF-17	300mm2 3x1C Cu R E 110 PVC	G9	TF-17	0.018
GN-10 - TF-18	300mm2 3x1C Cu R E 110 PVC	G10	TF-18	0.016
GN-11 - TF-18	300mm2 3x1C Cu R E 110 PVC	G11	TF-18	0.012
GN-12 - TF-19	300mm2 3x1C Cu R E 110 PVC	G12	TF-19	0.014
GN-13 - TF-19	300mm2 3x1C Cu R E 110 PVC	G13	TF-19	0.018
TF-01 - DB-101	300mm2 2x1C Cu XLPE PVC 0.6-1kV	TF01LV	DB101	0.025
TF-01 FDR	150mm2 3x1c Cu XLPE 6.35 11kV	TF01HV	SB001	0.025
TF-02 FDR	120mm2 6.35-11kV 3C Cu XLPE Screened PVC	SB001	TF02	0.4
TF-023 FDR	120mm2 6.35-11kV 3C Cu XLPE Screened PVC	SB001	TF23	0.05
TF-03 FDR	120mm2 6.35-11kV 3C Cu XLPE Screened PVC	SB001	TF03	0.5
TF-04 FDR	120mm2 6.35-11kV 3C Cu XLPE Screened PVC	SB001	TF04	0.4
TF-05 FDR	120mm2 6.35-11kV 3C Cu XLPE Screened PVC	SB001	TF05	0.1
TF-07 FDR	120mm2 6.35-11kV 3C Cu XLPE Screened PVC	SB001	TF07	0.05
TF-11 - SB001	150mm2 3x1c Cu XLPE 6.35 11kV	TF11	SB001	0.081
TF-13 - SB001	150mm2 3x1c Cu XLPE 6.35 11kV	TF13	SB001	0.061
TF-13 - TF-12	150mm2 3x1c Cu XLPE 6.35 11kV	TF13	TF12	0.012
TF-15 - SB001	150mm2 3x1c Cu XLPE 6.35 11kV	TF15	SB001	0.045
TF-15 - TF-14	150mm2 3x1c Cu XLPE 6.35 11kV	TF14	TF15	0.012
TF-17 - SB001	150mm2 3x1c Cu XLPE 6.35 11kV	TF17	SB001	0.076
TF-17 - TF-16	150mm2 3x1c Cu XLPE 6.35 11kV	TF16	TF17	0.012
TF-19 - SB001	150mm2 3x1c Cu XLPE 6.35 11kV	TF19	SB001	0.047
TF-19 -TF-18	150mm2 3x1c Cu XLPE 6.35 11kV	TF18	TF19	0.012
TF-20 FDR	150mm2 3x1c Cu XLPE 6.35 11kV	TF20	SB001	0.025
TF-21 - HPGR1a	240mm2 6.35-11kV 3C Cu XLPE Screen HPGR	TF21A2	TF21A1	0.125
TF-21 - HPGR1b	240mm2 6.35-11kV 3C Cu XLPE Screen HPGR	TF21B2	TF21B1	0.125
TF-21 FDR	185mm2 6.35-11kV 3C Cu XLPE Screened PVC	SB001	TF21	0.4
TF-22 - HPGR2a	240mm2 6.35-11kV 3C Cu XLPE Screen HPGR	TF22A1	TF22A2	0.125
TF-22 - HPGR2b	240mm2 6.35-11kV 3C Cu XLPE Screen HPGR	TF22B1	TF22B2	0.125
TF-22 FDR	185mm2 6.35-11kV 3C Cu XLPE Screened PVC	SB001	TF22	0.4
TF-23a	240mm2 6.35-11kV 3C Cu XLPE Screened PVC	TF23A2	TF23A1	0.125
TF-23b	240mm2 6.35-11kV 3C Cu XLPE Screened PVC	TF23B1	TF23B2	0.125

Electrical Load Information

EQUIPMENT NAME		INSTALLED MOTOR POWER (kW)	Fiixed or Variable Speed	Plant Area	LV MCC no. or Switch Room no.	INSTALLED POWER (kW) * Formula use only*	Remarks on motor & motor cables	MCC circuit type	LV motor schematic no. (DR-EL-)
MAXIMUM DEMAND CALCULATIONS		Maximum Demand ("Duty" loads only) @ 100% nameplate ratings	(kW)	Maximum Demand @ 100% nameplate ratings & 0.90 power factor	(kVA)	Maximum Demand @ 70% utilisation factor & 0.90 power factor	(kVA)	Maximum Demand @ 70% utilisation factor & 0.90 power factor	(kW)
TF-002 for HPGR switchroom SR-002 & LV MCC-002		2463	kW	2737	kVA	1916	kVA	1724	kW
TF-021 for HPGR Fixed Roll main drive VSD & HV motor		2898	kW	3220	kVA	2254	kVA	2029	kW
TF-022 for HPGR Movable Roll main drive VSD & HV motor		2898	kW	3220	kVA	2254	kVA	2029	kW
TF-003 for DMS switchroom SR-003 & LV MCC-003		2084	kW	2316	kVA	1621	kVA	1459	kW
TF-004 for Crushing & Screening switchroom SR-004 & LV MCC-004		3142	kW	3491	kVA	2444	kVA	2199	kW
TF-005 for WMS switchroom SR-005 & LV MCC-005		1758	kW	1953	kVA	1367	kVA	1231	kW
TF-007 for Slurry Transfer switchroom SR-007 & LV MCC-007		1731	kW	1923	kVA	1346	kVA	1212	kW
TF-023 for Slurry Transfer Geho PD Pump PU-061 VSD & HV motor		2000	kW	2222	kVA	1556	kVA	1400	kW
Total (Main Plant)		18974	kW	21082	kVA	14758	kVA	13282	kW

Figure 11: Electrical Load List - Maximum Demand

Table 14: Asynchronous Motor Loads

Name	Busbar	Bus T.	Act.Pow.	React.Pow.	App.Pow.	Pow.Fact.	cos(phi) (ind,cap)	Voltage
			MW	Mvar	MVA			p.u.
DOL 103.27kW	MCC-002	PQ	0.072	0.045	0.085	0.85	ind.	1
L-DOL 75kW	MCC-002	PQ	0.075	0.046	0.088	0.85	ind.	1
DOL 324kW	MCC-003	PQ	0.226	0.140	0.266	0.85	ind.	1
L-DOL 150kW	MCC-003	PQ	0.150	0.093	0.176	0.85	ind.	1
SS 560kW	MCC-003	PQ	0.392	0.243	0.461	0.85	ind.	1
DOL 510kW	MCC-004	PQ	0.306	0.190	0.360	0.85	ind.	1
L-DOL 45kW(1)	MCC-004	PQ	0.045	0.028	0.053	0.85	ind.	1
SS 2200kW	MCC-004	PQ	1.320	0.818	1.553	0.85	ind.	1
DOL 268.25kW	MCC-005	PQ	0.188	0.116	0.221	0.85	ind.	1
L-DOL 45kW	MCC-005	PQ	0.045	0.028	0.053	0.85	ind.	1
SS 355kW	MCC-005	PQ	0.249	0.154	0.292	0.85	ind.	1
DOL 160kW	MCC-007	PQ	0.112	0.069	0.132	0.85	ind.	1
L-DOL 90kW	MCC-007	PQ	0.090	0.056	0.106	0.85	ind.	1
SS 710kW	MCC-007	PQ	0.497	0.308	0.585	0.85	ind.	1

Table 15: General and VSD Loads

Name	Terminal	Act.Pow.	React. Pow.	App. Pow.	I(rated)	Pow.Fact.	cos(phi) (ind,cap)	Voltage
		MW	Mvar	MVA	kA			p.u.
Auxiliary DB102 - Static 20kW	DB101	0.020	0.010	0.022	0.031	0.9	ind.	1
Static 60kW	DB101	0.060	0.029	0.067	0.093	0.9	ind.	1
Static 260kW	MCC-002	0.182	0.088	0.202	0.281	0.9	ind.	1
VSD 2.025MW	MCC-002	1.418	0.560	1.524	2.120	0.93	ind.	1
Static 230kW	MCC-003	0.161	0.078	0.179	0.249	0.9	ind.	1
VSD 820kW	MCC-003	0.574	0.227	0.617	0.859	0.93	ind.	1
Static 155kW	MCC-004	0.109	0.053	0.121	0.168	0.9	ind.	1
VSD 100kW	MCC-004	0.060	0.024	0.065	0.090	0.93	ind.	1
Static 255kW	MCC-005	0.179	0.086	0.198	0.276	0.9	ind.	1
VSD 775kW	MCC-005	0.543	0.214	0.583	0.812	0.93	ind.	1
Static 395kW	MCC-007	0.277	0.134	0.307	0.427	0.9	ind.	1
VSD 595kW	MCC-007	0.417	0.165	0.448	0.623	0.93	ind.	1
HPGR 1a	TF21A2	1.014	0.401	1.091	0.331	0.93	ind.	1
HPGR 1b	TF21B2	1.014	0.401	1.091	0.331	0.93	ind.	1
HPGR 2a	TF22A2	1.014	0.401	1.091	0.331	0.93	ind.	1
HPGR 2b	TF22B2	1.014	0.401	1.091	0.331	0.93	ind.	1
Overland Pipeline Pump A	TF23A2	0.689	0.272	0.741	0.194	0.93	ind.	1
Overland Pipeline Pump B	TF23B2	0.689	0.272	0.741	0.194	0.93	ind.	1

Appendix C: Load Flow Results

Table 16: Terminal Voltages

Name	Nom.L-L Volt.	Ul, Magnitude	u, Magnitude	U, Angle
	kV	kV	p.u.	deg
DB101	0.415	0.413	0.994	-32.826
G1	0.415	0.430	1.037	0.000
G2	0.415	0.431	1.037	0.012
G3	0.415	0.430	1.037	0.001
G4	0.415	0.431	1.037	0.012
G5	0.415	0.430	1.037	0.000
G6	0.415	0.431	1.038	-0.008
G7	0.415	0.431	1.038	-0.025
G8	0.415	0.431	1.038	-0.017
G9	0.415	0.431	1.039	-0.001
G10	0.415	0.431	1.038	-0.011
G11	0.415	0.430	1.037	-0.027
G12	0.415	0.000	0.000	0.000
G13	0.415	0.000	0.000	0.000
TF-11 415V 85kA 1s	0.415	0.429	1.034	-0.057
TF-12 415V 85kA 1s	0.415	0.429	1.034	-0.056
TF-13 415V 85kA 1s	0.415	0.429	1.034	-0.056
TF-14 415V 85kA 1s	0.415	0.429	1.034	-0.057
TF-15 415V 85kA 1s	0.415	0.429	1.034	-0.056
TF-16 415V 85kA 1s	0.415	0.429	1.035	-0.074
TF-17 415V 85kA 1s	0.415	0.429	1.035	-0.075
TF-18 415V 85kA 1s	0.415	0.429	1.035	-0.077
TF-19 415V 85kA 1s	0.415	0.415	0.999	-2.489
TF11	11	11.002	1.000	-32.490
TF12	11	11.004	1.000	-32.488
TF13	11	11.003	1.000	-32.488
TF14	11	11.003	1.000	-32.489
TF15	11	11.002	1.000	-32.489
TF16	11	11.005	1.000	-32.486
TF17	11	11.005	1.000	-32.486
TF18	11	11.002	1.000	-32.490
TF19	11	11.002	1.000	-32.490
TF20	11	11.000	1.000	-32.492
SB001	11	11.000	1.000	-32.492
TF01HV	11	11.000	1.000	-32.492
TF01LV	0.415	0.413	0.995	-32.809
TF02	11	10.987	0.999	-32.500
TF03	11	10.985	0.999	-32.495
TF04	11	10.985	0.999	-32.490

Name	Nom.L-L Volt.	Ul, Magnitude	u, Magnitude	U, Angle
TF05	11	10.998	1.000	-32.493
TF07	11	10.999	1.000	-32.493
MCC-002	0.415	0.401	0.965	-5.474
MCC-003	0.415	0.401	0.965	-5.018
MCC-004	0.415	0.395	0.952	-5.579
MCC-005	0.415	0.404	0.974	-4.496
MCC-007	0.415	0.402	0.969	-4.814
TF21	11	10.989	0.999	-32.510
TF21A1	1.903	1.823	0.958	-5.995
TF21A2	1.903	1.815	0.954	-6.119
TF21B1	1.903	1.823	0.958	-35.995
TF21B2	1.903	1.815	0.954	-36.119
TF22	11	10.989	0.999	-32.510
TF22A1	1.903	1.823	0.958	-5.995
TF22A2	1.903	1.815	0.954	-6.119
TF22B1	1.903	1.823	0.958	-35.995
TF22B2	1.903	1.815	0.954	-36.119
TF23	11	10.999	1.000	-32.493
TF23A1	2.2	2.104	0.957	-35.310
TF23A2	2.2	2.100	0.954	-35.373
TF23B1	2.2	2.104	0.956	-5.322
TF23B2	2.2	2.100	0.954	-5.385

Table 17: Cable Loading

Name	Terminal i	Terminal j	u, Magnitude	u, Magnitude	Loading
	Busbar	Busbar	Terminal i in p.u.	Terminal j in p.u.	%
GN-01 - TF-11	G1	TF-11 415V 85kA 1s	1.037	1.034	67.281
GN-02 - TF-12	G2	TF-12 415V 85kA 1s	1.037	1.034	67.235
GN-03 - TF-13	G3	TF-13 415V 85kA 1s	1.037	1.034	67.276
GN-04 - TF-14	G4	TF-14 415V 85kA 1s	1.037	1.034	67.240
GN-05 - TF-15	G5	TF-15 415V 85kA 1s	1.037	1.034	67.280
GN-06 - TF-16	G6	TF-16 415V 85kA 1s	1.038	1.035	70.331
GN-07 - TF-16	G7	TF-16 415V 85kA 1s	1.038	1.035	70.390
GN-08 - TF-17	G8	TF-17 415V 85kA 1s	1.038	1.035	70.364
GN-09 - TF-17	G9	TF-17 415V 85kA 1s	1.039	1.035	70.305
GN-10 - TF-18	G10	TF-18 415V 85kA 1s	1.038	1.035	70.352
GN-11 - TF-18	G11	TF-18 415V 85kA 1s	1.037	1.035	70.411
GN-12 - TF-19	G12	- TF-19 415V 85kA 1s	0.000	0.000	0.000
GN-13 - TF-19	G13	- TF-19 415V 85kA 1s	0.000	0.000	0.000
TF-01 - DB-101	TF01LV	DB101	0.995	0.994	8.519
TF-01 FDR	TF01HV	SB001	1.000	1.000	1.313
TF-02 FDR	SB001	TF02	1.000	0.999	32.440
TF-023 FDR	SB001	TF23	1.000	1.000	25.956
TF-03 FDR	SB001	TF03	1.000	0.999	29.029
TF-04 FDR	SB001	TF04	1.000	0.999	37.281
TF-05 FDR	SB001	TF05	1.000	1.000	22.857
TF-07 FDR	SB001	TF07	1.000	1.000	26.868
TF-11 - SB001	TF11	SB001	1.000	1.000	23.263
TF-13 - SB001	TF13	SB001	1.000	1.000	46.507
TF-13 - TF-12	TF13	TF12	1.000	1.000	23.246
TF-15 - SB001	TF15	SB001	1.000	1.000	46.510
TF-15 - TF-14	TF14	TF15	1.000	1.000	23.248
TF-17 - SB001	TF17	SB001	1.000	1.000	58.376
TF-17 - TF-16	TF16	TF17	1.000	1.000	29.194
TF-19 - SB001	TF19	SB001	1.000	1.000	28.987
TF-19 -TF-18	TF18	TF19	1.000	1.000	29.202
TF-20 FDR	TF20	SB001	1.000	1.000	0.000
TF-21 - HPGR1a	TF21A2	TF21A1	0.954	0.958	77.977
TF-21 - HPGR1b	TF21B2	TF21B1	0.954	0.958	77.977
TF-21 FDR	SB001	TF21	1.000	0.999	29.934
TF-22 - HPGR2a	TF22A1	TF22A2	0.958	0.954	77.977
TF-22 - HPGR2b	TF22B1	TF22B2	0.958	0.954	77.977
TF-22 FDR	SB001	TF22	1.000	0.999	29.934
TF-23a	TF23A2	TF23A1	0.954	0.957	45.762
TF-23b	TF23B1	TF23B2	0.956	0.954	45.766

Table 18: 2 Winding Transformer Loading

Name	HV-Side	LV-Side	u, Magnitude	u, Magnitude	Loading
	Busbar	Busbar	HV-Side in p.u.	LV-Side in p.u.	%
TF-01	TF01HV	TF01LV	1.000	0.995	18.756
TF-02	TF02	MCC-002 ---- 4000A 65kA 1s	0.999	0.965	79.111
TF-03	TF03	MCC-003 ---- 4000A 65kA 1s	0.999	0.965	70.793
TF-04	TF04	MCC-004 ---- 4000A 65kA 1s	0.999	0.952	90.918
TF-05	TF05	MCC-005 ---- 4000A 65kA 1s	1.000	0.974	55.743
TF-07	TF07	MCC-007 ---- 4000A 65kA 1s	1.000	0.969	65.524
TF-11	TF11	TF-11 415V 85kA 1s	1.000	1.034	88.260
TF-12	TF12	TF-12 415V 85kA 1s	1.000	1.034	88.200
TF-13	TF13	TF-13 415V 85kA 1s	1.000	1.034	88.253
TF-14	TF14	TF-14 415V 85kA 1s	1.000	1.034	88.206
TF-15	TF15	TF-15 415V 85kA 1s	1.000	1.034	88.259
TF-16	TF16	TF-16 415V 85kA 1s	1.000	1.035	88.608
TF-17	TF17	TF-17 415V 85kA 1s	1.000	1.035	88.575
TF-18	TF18	TF-18 415V 85kA 1s	1.000	1.035	88.634
TF-19	TF19	TF-19 415V 85kA 1s	1.000	0.999	1.199

Table 19: 3 Winding Transformer Loading

Name	HV-Side	MV-Side	LV-Side	u, Magnitude	u, Magnitude	u, Magnitude	Maximum Loading
	Busbar	Busbar	Busbar	HV-Side in p.u.	MV-Side in p.u.	LV-Side in p.u.	%
TF-23	TF23	TF23A1	TF23B1	1.000	0.957	0.956	65.938
TF-21	TF21	TF21A1	TF21B1	0.999	0.958	0.958	64.992
TF-22	TF22	TF22A1	TF22B1	0.999	0.958	0.958	64.992

Appendix D: Short Circuit Results

Max. Three-Phase Faults

Complete Method

Table 20: Busbar Loading Max 3ϕ Complete

Name	Type	Ik"	ip	Loading, Ip	Ith	Loading, Ith
		kA	kA	%	kA	%
TF-11 415V 85kA 1s	Busbar	59.596	142.924	67.258	60.412	71.073
TF-12 415V 85kA 1s	Busbar	59.504	142.499	67.058	60.311	70.954
TF-13 415V 85kA 1s	Busbar	59.633	143.086	67.335	60.452	71.120
TF-14 415V 85kA 1s	Busbar	59.513	142.544	67.080	60.321	70.966
TF-15 415V 85kA 1s	Busbar	59.642	143.132	67.356	60.462	71.132
TF-16 415V 85kA 1s	Busbar	70.391	167.015	78.595	71.290	83.871
TF-17 415V 85kA 1s	Busbar	70.314	166.679	78.437	71.207	83.773
TF-18 415V 85kA 1s	Busbar	70.386	167.015	78.596	71.286	83.865
TF-19 415V 85kA 1s	Busbar	42.156	98.280	46.249	42.640	50.165
SB001 ------ 1250A 25kA 1s	Busbar	6.579	15.249	24.398	5.866	23.465
DB101	Busbar	14.624	30.331	0.000	14.720	0.000
MCC-002 ---- 4000A 65kA 1s	Busbar	36.986	84.978	52.294	37.376	57.502
MCC-003 ---- 4000A 65kA 1s	Busbar	42.477	94.622	58.229	39.083	60.128
MCC-004 ---- 4000A 65kA 1s	Busbar	53.949	115.744	71.227	46.119	70.953
MCC-005 ---- 4000A 65kA 1s	Busbar	40.434	92.192	56.733	40.844	62.837
MCC-007 ---- 4000A 65kA 1s	Busbar	44.851	100.413	61.792	40.757	62.703
TF01HV	Junction Node	6.555	15.149	0.000	5.846	0.000
TF01LV	Junction Node	15.809	34.009	0.000	15.929	0.000
TF02	Junction Node	6.239	13.681	0.000	5.571	0.000
TF03	Junction Node	6.179	13.416	0.000	5.516	0.000
TF04	Junction Node	6.283	13.859	0.000	5.601	0.000
TF05	Junction Node	6.494	14.837	0.000	5.791	0.000
TF07	Junction Node	6.538	15.048	0.000	5.830	0.000
TF20	Junction Node	6.555	15.149	0.000	5.846	0.000
TF21	Junction Node	6.283	14.053	0.000	5.613	0.000
TF21A2	Junction Node	5.606	11.911	0.000	5.647	0.000
TF21B2	Junction Node	5.606	11.911	0.000	5.647	0.000
TF22	Junction Node	6.283	14.053	0.000	5.613	0.000
TF22A2	Junction Node	5.606	11.911	0.000	5.647	0.000
TF22B2	Junction Node	5.606	11.911	0.000	5.647	0.000
TF23	Junction Node	6.534	15.032	0.000	5.827	0.000
TF23A2	Junction Node	3.875	7.594	0.000	3.895	0.000
TF23B2	Junction Node	3.860	7.574	0.000	3.881	0.000

Table 21: Cable Loading Max 3ϕ Complete

Name	Nominal Current	ip	Ithr(1s)	Ithmax	Loading
	kA		kA	kA	%
GN-01 - TF-11	3.650	60.545	198.000	60.412	30.511
GN-02 - TF-12	3.650	60.183	198.000	60.311	30.460
GN-03 - TF-13	3.650	60.581	198.000	60.452	30.531
GN-04 - TF-14	3.650	60.189	198.000	60.321	30.465
GN-05 - TF-15	3.650	60.588	198.000	60.462	30.536
GN-06 - TF-16	2.190	35.487	118.800	71.290	60.009
GN-07 - TF-16	2.190	35.705	118.800	71.290	60.009
GN-08 - TF-17	2.190	35.562	118.800	71.207	59.938
GN-09 - TF-17	2.190	35.346	118.800	71.207	59.938
GN-10 - TF-18	2.190	35.481	118.800	71.286	60.005
GN-11 - TF-18	2.190	35.699	118.800	71.286	60.005
GN-12 - TF-19	2.190	0.000	118.800	0.000	0.000
GN-13 - TF-19	2.190	0.000	118.800	0.000	0.000
TF-01 - DB-101	1.460	30.331	79.200	15.929	20.113
TF-01 FDR	0.375	0.000	21.450	5.866	27.348
TF-02 FDR	0.320	13.588	17.200	5.866	34.106
TF-023 FDR	0.320	15.032	17.200	5.866	34.106
TF-03 FDR	0.320	12.938	17.200	5.866	34.106
TF-04 FDR	0.320	12.817	17.200	5.866	34.106
TF-05 FDR	0.320	14.488	17.200	5.866	34.106
TF-07 FDR	0.320	14.410	17.200	5.866	34.106
TF-11 - SB001	0.395	1.456	21.450	5.866	27.348
TF-13 - SB001	0.395	2.906	21.450	5.866	27.348
TF-13 - TF-12	0.395	13.614	21.450	5.834	27.200
TF-15 - SB001	0.395	2.907	21.450	5.866	27.348
TF-15 - TF-14	0.395	1.448	21.450	5.843	27.239
TF-17 - SB001	0.395	3.518	21.450	5.866	27.348
TF-17 - TF-16	0.395	1.756	21.450	5.832	27.189
TF-19 - SB001	0.395	1.763	21.450	5.866	27.348
TF-19 -TF-18	0.395	1.757	21.450	5.836	27.209
TF-20 FDR	0.395	0.000	21.450	5.866	27.348
TF-21 - HPGR1a	0.445	0.000	34.300	6.059	17.663
TF-21 - HPGR1b	0.445	0.000	34.300	6.059	17.663
TF-21 FDR	0.405	14.053	26.500	5.866	22.137
TF-22 - HPGR2a	0.445	11.911	34.300	6.059	17.663
TF-22 - HPGR2b	0.445	11.911	34.300	6.059	17.663
TF-22 FDR	0.405	14.053	26.500	5.866	22.137
TF-23a	0.445	0.000	34.300	4.066	11.853
TF-23b	0.445	7.574	34.300	4.050	11.807

IEC60909 Method (for comparison)

Table 22: Busbar Loading Max 3ϕ IEC60909

Name	Type	Ik"	ip	Loading, Ip	Ith	Loading, Ith
		kA	kA	%	kA	%
DB101	Busbar	15.667	32.362	0.000	14.433	0.000
MCC-002 ---- 4000A 65kA 1s	Busbar	39.994	91.035	56.022	36.691	56.448
MCC-003 ---- 4000A 65kA 1s	Busbar	46.793	103.436	63.653	41.178	63.351
MCC-004 ---- 4000A 65kA 1s	Busbar	61.030	130.214	80.132	49.699	76.459
MCC-005 ---- 4000A 65kA 1s	Busbar	44.226	100.029	61.556	39.655	61.008
MCC-007 ---- 4000A 65kA 1s	Busbar	49.510	110.079	67.741	43.075	66.269
SB001 ----- 1250A 25kA 1s	Busbar	7.096	15.784	25.255	6.556	26.225
TF-11 415V 85kA 1s	Busbar	60.920	140.492	66.114	61.577	72.444
TF-12 415V 85kA 1s	Busbar	60.815	140.112	65.935	61.468	72.315
TF-13 415V 85kA 1s	Busbar	60.952	140.641	66.184	61.612	72.484
TF-14 415V 85kA 1s	Busbar	60.827	140.167	65.961	61.481	72.330
TF-15 415V 85kA 1s	Busbar	60.964	140.695	66.210	61.625	72.500
TF-16 415V 85kA 1s	Busbar	73.199	167.910	79.016	73.966	87.019
TF-17 415V 85kA 1s	Busbar	73.118	167.614	78.877	73.881	86.919
TF-18 415V 85kA 1s	Busbar	73.211	167.952	79.036	73.979	87.034
TF-19 415V 85kA 1s	Busbar	45.336	104.545	49.198	41.984	49.392
TF01HV	Junction Node	7.072	15.688	0.000	6.533	0.000
TF01LV	Junction Node	16.960	36.352	0.000	15.645	0.000
TF02	Junction Node	6.753	14.259	0.000	6.225	0.000
TF03	Junction Node	6.703	14.026	0.000	6.172	0.000
TF04	Junction Node	6.816	14.479	0.000	6.276	0.000
TF05	Junction Node	7.013	15.389	0.000	6.475	0.000
TF07	Junction Node	7.057	15.593	0.000	6.517	0.000
TF20	Junction Node	7.072	15.688	0.000	6.533	0.000
TF21	Junction Node	6.790	14.612	0.000	6.264	0.000
TF21A2	Junction Node	6.149	12.986	0.000	5.669	0.000
TF21B2	Junction Node	6.149	12.986	0.000	5.669	0.000
TF22	Junction Node	6.790	14.612	0.000	6.264	0.000
TF22A2	Junction Node	6.149	12.986	0.000	5.669	0.000
TF22B2	Junction Node	6.149	12.986	0.000	5.669	0.000
TF23	Junction Node	7.051	15.574	0.000	6.513	0.000
TF23A2	Junction Node	4.247	8.287	0.000	3.907	0.000
TF23B2	Junction Node	4.232	8.266	0.000	3.893	0.000

Table 23: Cable Loading Max 3ϕ IEC60909

Name	Nominal Current	ip	Ithr(1s)	Ithmax	Loading
	kA	Terminal j in kA	kA	kA	%
GN-01 - TF-11	3.650	56.912	198.000	61.577	31.099
GN-02 - TF-12	3.650	56.555	198.000	61.468	31.044
GN-03 - TF-13	3.650	56.942	198.000	61.612	31.117
GN-04 - TF-14	3.650	56.565	198.000	61.481	31.051
GN-05 - TF-15	3.650	56.952	198.000	61.625	31.124
GN-06 - TF-16	2.190	33.479	118.800	73.966	62.261
GN-07 - TF-16	2.190	33.716	118.800	73.966	62.261
GN-08 - TF-17	2.190	33.575	118.800	73.881	62.190
GN-09 - TF-17	2.190	33.339	118.800	73.881	62.190
GN-10 - TF-18	2.190	33.481	118.800	73.979	62.272
GN-11 - TF-18	2.190	33.719	118.800	73.979	62.272
GN-12 - TF-19	2.190	0.000	118.800	0.000	0.000
GN-13 - TF-19	2.190	0.000	118.800	0.000	0.000
TF-01 - DB-101	1.460	32.362	79.200	15.645	19.753
TF-01 FDR	0.375	0.000	21.450	6.556	30.565
TF-02 FDR	0.320	14.136	17.200	6.556	38.118
TF-023 FDR	0.320	15.574	17.200	6.556	38.118
TF-03 FDR	0.320	13.406	17.200	6.556	38.118
TF-04 FDR	0.320	13.130	17.200	6.556	38.118
TF-05 FDR	0.320	14.950	17.200	6.556	38.118
TF-07 FDR	0.320	14.798	17.200	6.556	38.118
TF-11 - SB001	0.395	1.439	21.450	6.556	30.565
TF-13 - SB001	0.395	2.870	21.450	6.556	30.565
TF-13 - TF-12	0.395	14.176	21.450	6.521	30.399
TF-15 - SB001	0.395	2.871	21.450	6.556	30.565
TF-15 - TF-14	0.395	1.430	21.450	6.530	30.443
TF-17 - SB001	0.395	3.464	21.450	6.556	30.565
TF-17 - TF-16	0.395	1.730	21.450	6.517	30.385
TF-19 - SB001	0.395	1.736	21.450	6.556	30.565
TF-19 -TF-18	0.395	1.731	21.450	6.523	30.409
TF-20 FDR	0.395	0.000	21.450	6.556	30.565
TF-21 - HPGR1a	0.445	0.000	34.300	6.073	17.705
TF-21 - HPGR1b	0.445	0.000	34.300	6.073	17.705
TF-21 FDR	0.405	14.612	26.500	6.556	24.740
TF-22 - HPGR2a	0.445	12.986	34.300	6.073	17.705
TF-22 - HPGR2b	0.445	12.986	34.300	6.073	17.705
TF-22 FDR	0.405	14.612	26.500	6.556	24.740
TF-23a	0.445	0.000	34.300	4.074	11.878
TF-23b	0.445	8.266	34.300	4.059	11.834

Min. Three Phase Faults (Complete Method)

Table 24: Busbar Loading Min 3ϕ

Name	Type	Ik" A	ip A	Loading, Ip	Ithmax	Loading, Ith
		kA	kA	%	kA	%
DB101	Busbar	7.966	16.599	0.000	8.019	0.000
MCC-002 ---- 4000A 65kA 1s	Busbar	15.121	35.230	21.680	15.294	23.529
MCC-003 ---- 4000A 65kA 1s	Busbar	14.936	34.683	21.344	15.104	23.237
MCC-004 ---- 4000A 65kA 1s	Busbar	14.873	34.651	21.324	15.043	23.143
MCC-005 ---- 4000A 65kA 1s	Busbar	15.069	35.467	21.826	15.252	23.464
MCC-007 ---- 4000A 65kA 1s	Busbar	15.083	35.561	21.884	15.268	23.489
SB001 -------- 1250A 25kA 1s	Busbar	1.091	2.585	4.135	1.105	4.421
TF-11 415V 85kA 1s	Busbar	14.842	35.013	16.477	15.025	17.677
TF-12 415V 85kA 1s	Busbar	14.845	35.027	16.483	15.028	17.680
TF-13 415V 85kA 1s	Busbar	14.849	35.048	16.493	15.033	17.685
TF-14 415V 85kA 1s	Busbar	14.850	35.055	16.496	15.034	17.687
TF-15 415V 85kA 1s	Busbar	14.854	35.076	16.506	15.038	17.692
TF-16 415V 85kA 1s	Busbar	16.367	38.561	18.146	16.568	19.491
TF-17 415V 85kA 1s	Busbar	24.254	57.361	26.993	24.558	28.892
TF-18 415V 85kA 1s	Busbar	33.137	79.031	37.191	33.574	39.499
TF-19 415V 85kA 1s	Busbar	16.385	38.653	18.190	16.587	19.514
TF01HV	Junction Node	1.090	2.579	0.000	1.104	0.000
TF01LV	Junction Node	8.571	18.986	0.000	8.646	0.000
TF02	Junction Node	1.072	2.483	0.000	1.084	0.000
TF03	Junction Node	1.066	2.455	0.000	1.077	0.000
TF04	Junction Node	1.070	2.479	0.000	1.082	0.000
TF05	Junction Node	1.086	2.558	0.000	1.100	0.000
TF07	Junction Node	1.089	2.571	0.000	1.102	0.000
TF20	Junction Node	1.090	2.579	0.000	1.104	0.000
TF21	Junction Node	1.076	2.513	0.000	1.089	0.000
TF21A2	Junction Node	2.653	5.721	0.000	2.674	0.000
TF21B2	Junction Node	2.653	5.721	0.000	2.674	0.000
TF22	Junction Node	1.076	2.513	0.000	1.089	0.000
TF22A2	Junction Node	2.653	5.721	0.000	2.674	0.000
TF22B2	Junction Node	2.653	5.721	0.000	2.674	0.000
TF23	Junction Node	1.089	2.571	0.000	1.102	0.000
TF23A2	Junction Node	1.961	4.031	0.000	1.974	0.000
TF23B2	Junction Node	1.956	4.024	0.000	1.969	0.000

Table 25: Cable Loading Min 3ϕ

Name	Ik" A	ip A	Ithmax	Ithr(1s)	Loading
	Terminal j in kA	Terminal j in kA	kA	kA	%
GN-01 - TF-11	0.000	0.000	0.000	198.000	0.000
GN-02 - TF-12	0.000	0.000	0.000	198.000	0.000
GN-03 - TF-13	0.000	0.000	0.000	198.000	0.000
GN-04 - TF-14	0.000	0.000	0.000	198.000	0.000
GN-05 - TF-15	0.000	0.000	0.000	198.000	0.000
GN-06 - TF-16	0.000	0.000	0.000	118.800	0.000
GN-07 - TF-16	0.000	0.000	0.000	118.800	0.000
GN-08 - TF-17	0.000	0.000	0.000	118.800	0.000
GN-09 - TF-17	12.726	30.097	24.558	118.800	20.672
GN-10 - TF-18	12.774	30.466	30.908	118.800	26.017
GN-11 - TF-18	12.870	30.694	30.908	118.800	26.017
GN-12 - TF-19	0.000	0.000	0.000	118.800	0.000
GN-13 - TF-19	0.000	0.000	0.000	118.800	0.000
TF-01 - DB-101	7.966	16.599	8.646	79.200	10.916
TF-01 FDR	0.000	0.000	1.105	21.450	5.152
TF-02 FDR	1.072	2.483	1.105	17.200	6.426
TF-023 FDR	1.089	2.571	1.105	17.200	6.426
TF-03 FDR	1.066	2.455	1.105	17.200	6.426
TF-04 FDR	1.070	2.479	1.105	17.200	6.426
TF-05 FDR	1.086	2.558	1.105	17.200	6.426
TF-07 FDR	1.089	2.571	1.105	17.200	6.426
TF-11 - SB001	0.000	0.000	1.105	21.450	5.152
TF-13 - SB001	0.000	0.000	1.105	21.450	5.152
TF-13 - TF-12	1.088	2.567	1.102	21.450	5.137
TF-15 - SB001	0.000	0.000	1.105	21.450	5.152
TF-15 - TF-14	0.000	0.000	1.103	21.450	5.141
TF-17 - SB001	0.407	0.963	1.105	21.450	5.152
TF-17 - TF-16	0.000	0.000	1.103	21.450	5.144
TF-19 - SB001	0.685	1.621	1.105	21.450	5.152
TF-19 -TF-18	0.685	1.623	1.105	21.450	5.152
TF-20 FDR	0.000	0.000	1.105	21.450	5.152
TF-21 - HPGR1a	0.000	0.000	2.987	34.300	8.709
TF-21 - HPGR1b	0.000	0.000	2.987	34.300	8.709
TF-21 FDR	1.076	2.513	1.105	26.500	4.171
TF-22 - HPGR2a	2.793	6.022	2.987	34.300	8.709
TF-22 - HPGR2b	2.793	6.022	2.987	34.300	8.709
TF-22 FDR	1.076	2.513	1.105	26.500	4.171
TF-23a	0.000	0.000	2.160	34.300	6.296
TF-23b	2.059	4.235	2.154	34.300	6.280

Max. Single Line to Ground Faults (Complete Method)

Table 26: Busbar Loading Max 1ϕ

Name	Type	Ik" A	ip A	Loading, Ip	Ithmax	Loading, Ith
		kA	kA	%	kA	%
DB101	Busbar	15.736	32.637	0.000	15.839	0.000
MCC-002 ---- 4000A 65kA 1s	Busbar	41.134	94.510	58.160	41.569	63.952
MCC-003 ---- 4000A 65kA 1s	Busbar	45.629	101.643	62.549	46.040	70.830
MCC-004 ---- 4000A 65kA 1s	Busbar	53.882	115.600	71.138	54.289	83.522
MCC-005 ---- 4000A 65kA 1s	Busbar	44.046	100.428	61.802	44.493	68.451
MCC-007 ---- 4000A 65kA 1s	Busbar	47.502	106.348	65.445	47.941	73.755
SB001 ------1250A 25kA 1s	Busbar	0.100	0.232	0.371	0.101	0.404
TF-11 415V 85kA 1s	Busbar	55.107	132.159	62.192	55.862	65.720
TF-12 415V 85kA 1s	Busbar	55.072	131.884	62.063	55.819	65.669
TF-13 415V 85kA 1s	Busbar	55.131	132.285	62.252	55.889	65.752
TF-14 415V 85kA 1s	Busbar	55.076	131.917	62.079	55.824	65.675
TF-15 415V 85kA 1s	Busbar	55.136	132.318	62.267	55.894	65.758
TF-16 415V 85kA 1s	Busbar	66.411	157.571	74.151	67.259	79.128
TF-17 415V 85kA 1s	Busbar	66.376	157.344	74.044	67.219	79.081
TF-18 415V 85kA 1s	Busbar	66.402	157.562	74.147	67.251	79.118
TF-19 415V 85kA 1s	Busbar	47.197	110.032	51.780	47.739	56.164
TF01HV	Junction Node	0.100	0.231	0.000	0.101	0.000
TF01LV	Junction Node	17.078	36.739	0.000	17.208	0.000
TF02	Junction Node	0.100	0.218	0.000	0.100	0.000
TF03	Junction Node	0.099	0.216	0.000	0.100	0.000
TF04	Junction Node	0.100	0.220	0.000	0.100	0.000
TF05	Junction Node	0.100	0.228	0.000	0.101	0.000
TF07	Junction Node	0.100	0.230	0.000	0.101	0.000
TF20	Junction Node	0.100	0.231	0.000	0.101	0.000
TF21	Junction Node	0.100	0.223	0.000	0.101	0.000
TF21A2	Junction Node	0.000	0.000	0.000	0.000	0.000
TF21B2	Junction Node	0.000	0.000	0.000	0.000	0.000
TF22	Junction Node	0.100	0.223	0.000	0.101	0.000
TF22A2	Junction Node	0.000	0.000	0.000	0.000	0.000
TF22B2	Junction Node	0.000	0.000	0.000	0.000	0.000
TF23	Junction Node	0.100	0.230	0.000	0.101	0.000
TF23A2	Junction Node	0.000	0.000	0.000	0.000	0.000
TF23B2	Junction Node	0.000	0.000	0.000	0.000	0.000

Table 27: Cable Loading Max 1ϕ

Name	Ik" A	ip A	Ithmax	Ithr(1s)	Loading
	Terminal j in kA	Terminal j in kA	kA	kA	%
GN-01 - TF-11	14.889	35.707	55.862	198.000	28.213
GN-02 - TF-12	14.841	35.542	55.819	198.000	28.191
GN-03 - TF-13	14.888	35.722	55.889	198.000	28.227
GN-04 - TF-14	14.840	35.544	55.824	198.000	28.194
GN-05 - TF-15	14.886	35.724	55.894	198.000	28.229
GN-06 - TF-16	9.079	21.542	67.259	118.800	56.615
GN-07 - TF-16	9.123	21.647	67.259	118.800	56.615
GN-08 - TF-17	9.103	21.579	67.219	118.800	56.581
GN-09 - TF-17	9.059	21.475	67.219	118.800	56.581
GN-10 - TF-18	9.076	21.537	67.251	118.800	56.608
GN-11 - TF-18	9.121	21.642	67.251	118.800	56.608
GN-12 - TF-19	0.000	0.000	0.000	118.800	0.000
GN-13 - TF-19	0.000	0.000	0.000	118.800	0.000
TF-01 - DB-101	15.753	32.673	17.208	79.200	21.727
TF-01 FDR	0.005	0.011	0.101	21.450	0.471
TF-02 FDR	0.196	0.430	0.101	17.200	0.588
TF-023 FDR	0.177	0.407	0.101	17.200	0.588
TF-03 FDR	0.181	0.394	0.101	17.200	0.588
TF-04 FDR	0.202	0.445	0.101	17.200	0.588
TF-05 FDR	0.164	0.376	0.101	17.200	0.588
TF-07 FDR	0.175	0.402	0.101	17.200	0.588
TF-11 - SB001	0.097	0.225	0.101	21.450	0.471
TF-13 - SB001	0.194	0.450	0.101	21.450	0.471
TF-13 - TF-12	0.051	0.117	0.101	21.450	0.471
TF-15 - SB001	0.194	0.450	0.101	21.450	0.471
TF-15 - TF-14	0.097	0.224	0.101	21.450	0.471
TF-17 - SB001	0.243	0.563	0.101	21.450	0.471
TF-17 - TF-16	0.122	0.281	0.101	21.450	0.471
TF-19 - SB001	0.121	0.280	0.101	21.450	0.471
TF-19 -TF-18	0.122	0.281	0.101	21.450	0.471
TF-20 FDR	0.033	0.077	0.101	21.450	0.471
TF-21 - HPGR1a	0.347	0.767	0.000	34.300	0.000
TF-21 - HPGR1b	0.347	0.767	0.000	34.300	0.000
TF-21 FDR	0.214	0.478	0.101	26.500	0.381
TF-22 - HPGR2a	0.347	0.737	0.000	34.300	0.000
TF-22 - HPGR2b	0.347	0.737	0.000	34.300	0.000
TF-22 FDR	0.214	0.478	0.101	26.500	0.381
TF-23a	0.204	0.406	0.000	34.300	0.000
TF-23b	0.204	0.400	0.000	34.300	0.000

Min. Single Line to Ground Faults (Complete Method)

Table 28: Busbar Loading Min 1ϕ

Name	Type	Ik" A	ip A	Loading, Ip	Ithmax	Loading, Ith
		kA	kA	%	kA	%
DB101	Busbar	9.069	18.897	0.000	9.130	0.000
MCC-002 ---- 4000A 65kA 1s	Busbar	18.434	42.949	26.430	18.645	28.684
MCC-003 ---- 4000A 65kA 1s	Busbar	18.251	42.381	26.081	18.456	28.394
MCC-004 ---- 4000A 65kA 1s	Busbar	18.186	42.371	26.075	18.394	28.299
MCC-005 ---- 4000A 65kA 1s	Busbar	18.376	43.251	26.616	18.599	28.614
MCC-007 ---- 4000A 65kA 1s	Busbar	18.388	43.354	26.680	18.614	28.637
SB001 1250A 25kA 1s	Busbar	0.073	0.174	0.278	0.074	0.297
TF-11 415V 85kA 1s	Busbar	17.941	42.323	19.917	18.162	21.367
TF-12 415V 85kA 1s	Busbar	17.943	42.338	19.924	18.165	21.370
TF-13 415V 85kA 1s	Busbar	17.947	42.360	19.934	18.169	21.375
TF-14 415V 85kA 1s	Busbar	17.948	42.368	19.938	18.170	21.377
TF-15 415V 85kA 1s	Busbar	17.952	42.390	19.948	18.175	21.382
TF-16 415V 85kA 1s	Busbar	20.084	47.317	22.267	20.329	23.917
TF-17 415V 85kA 1s	Busbar	27.270	64.493	30.350	27.612	32.484
TF-18 415V 85kA 1s	Busbar	34.508	82.301	38.730	34.964	41.134
TF-19 415V 85kA 1s	Busbar	20.101	47.419	22.315	20.349	23.939
TF01HV	Junction Node	0.073	0.174	0.000	0.074	0.000
TF01LV	Junction Node	9.783	21.672	0.000	9.869	0.000
TF02	Junction Node	0.073	0.169	0.000	0.074	0.000
TF03	Junction Node	0.073	0.168	0.000	0.074	0.000
TF04	Junction Node	0.073	0.169	0.000	0.074	0.000
TF05	Junction Node	0.073	0.173	0.000	0.074	0.000
TF07	Junction Node	0.073	0.173	0.000	0.074	0.000
TF20	Junction Node	0.073	0.174	0.000	0.074	0.000
TF21	Junction Node	0.073	0.171	0.000	0.074	0.000
TF21A2	Junction Node	0.000	0.000	0.000	0.000	0.000
TF21B2	Junction Node	0.000	0.000	0.000	0.000	0.000
TF22	Junction Node	0.073	0.171	0.000	0.074	0.000
TF22A2	Junction Node	0.000	0.000	0.000	0.000	0.000
TF22B2	Junction Node	0.000	0.000	0.000	0.000	0.000
TF23	Junction Node	0.073	0.173	0.000	0.074	0.000
TF23A2	Junction Node	0.000	0.000	0.000	0.000	0.000
TF23B2	Junction Node	0.000	0.000	0.000	0.000	0.000

Table 29: Cable Loading Min 1ϕ

Name	Grid	Ik" A	ip A	Ithmax	Ithr(1s)	Loading
		Terminal j in kA	Terminal j in kA	kA	kA	%
GN-09 - TF-17	Grid	9.671149	22.87195	27.61153	118.8	23.24203
GN-10 - TF-18	Grid	9.198274	21.93785	34.96354	118.8	29.43059
GN-11 - TF-18	Grid	9.260824	22.08703	34.96354	118.8	29.43059
TF-01 - DB-101	Grid	9.078968	18.91773	9.868872	79.2	12.4607

All remaining cables are HV or are delta connected therefore produce little to no line to ground fault current (all less than 1% loaded)

Protection Settings

415V 2.5MVA GTCB – Masterpact NW40H2 Micrologic 5.0E & SEL-751A

SEL-751A Protection Relay

<u>Phase Overcurrent (50P/51P):</u>

Phase CT = 4000/5A
5P20 5VA

51P1P Phase Time Overcurrent Trip Pickup	*= 4.78 (3824A)*
51P1C TOC Curve Selection	*= C1 (IEC Standard Inverse)*
51P1TD TOC Time Dial	*= 0.22*
50P1P Maximum Phase Overcurrent Trip Pickup (amps)	*= 52.20 (41760A)*
50P1D Maximum Phase Overcurrent Trip Delay (seconds)	*= 0.00 seconds*

<u>Neutral Overcurrent (50N/51N):</u>

Neutral CT = 4000/1A 5P20 10VA

51N1P Time Overcurrent Trip Pickup	*= 0.26 (1040A)*
51N1C TOC Curve Selection	*= C1 (IEC Standard Inverse)*
51N1TD TOC Time Dial	*= 0.05*
50N1P Neutral Overcurrent Trip Pickup	*= 1.50 (6000A)*
50N1D Neutral Overcurrent Trip Delay	*= 0.00 seconds*

If after the GTCB has opened and the SEL-751A protection relay continues to see 2000 Amps or more on the neutral, it will issue a trip signal to trip all the GCB's via the Power Station Controller.

415V 2MVA GTCB – Masterpact NW40H2 Micrologic 5.0E & SEL-751A

SEL-751A Protection Relay

<u>Phase Overcurrent (50P/51P):</u>

Phase CT = 4000/5A 5P20 5VA

51P1P Phase Time Overcurrent Trip Pickup	*= 3.83 (3064A)*
51P1C TOC Curve Selection	*= C1 (IEC Standard Inverse)*
51P1TD TOC Time Dial	*= 0.22*
50P1P Maximum Phase Overcurrent Trip Pickup (amps)	*= 41.71 (33,368A)*
50P1D Maximum Phase Overcurrent Trip Delay (seconds)	*= 0.00 seconds*

<u>Neutral Overcurrent (50N/51N):</u>

Neutral CT = 4000/1A 5P20 10VA

51N1P Time Overcurrent Trip Pickup	*= 0.26 (1040A)*
51N1C TOC Curve Selection	*= C1 (IEC Standard Inverse)*
51N1TD TOC Time Dial	*= 0.05*

50N1P Neutral Overcurrent Trip Pickup = 1.50 (6000A)
50N1D Neutral Overcurrent Trip Delay = 0.00 seconds

If after the GTCB has opened and the SEL-751A protection relay continues to see 2000 Amps or more on the neutral, it will issue a trip signal to trip all the GCB's via the Power Station Controller.

11kV HPGR Drive Feeders – SEL-751A (Panel G7 and G8)

Phase CT = 250/5A 5P10 5VA

Phase Overcurrent (Group 1):
51P1P Phase Time Overcurrent Trip Pickup = 4.00 (200A)
51P1C TOC Curve Selection = C1 (IEC Standard Inverse)
51P1TD TOC Time Dial = 0.12

50P1P Maximum Phase Overcurrent Trip Pickup (amps) = 44.80 (2240A)
50P1D Maximum Phase Overcurrent Trip Delay (seconds) = 0.00 seconds
Phase Overcurrent (Group 2):
51P1P Phase Time Overcurrent Trip Pickup = 4.00 (200A)
51P1C TOC Curve Selection = C1 (IEC Standard Inverse)
51P1TD TOC Time Dial = 0.07

50P1P Maximum Phase Overcurrent Trip Pickup (amps) = 44.80 (2240A)
50P1D Maximum Phase Overcurrent Trip Delay (seconds) = 0.00 seconds

Residual Overcurrent
50G1P Residual Overcurrent Trip Pickup (amps) = 0.5 (30A)
50G1D Residual Overcurrent Trip Delay (seconds) = 0.30 seconds

11kV 2.5MVA Transformer Feeder – SEL-751A (Panel G9 to G18)
Phase CT = 200/5A 5P10 5VA

Phase Overcurrent
51P1P Phase Time Overcurrent Trip Pickup = 3.90 (156A)
51P1C TOC Curve Selection = C1 (IEC Standard Inverse)
51P1TD TOC Time Dial = 0.12

50P1P Maximum Phase Overcurrent Trip Pickup (amps) = 39.40 (1576A)
50P1D Maximum Phase Overcurrent Trip Delay (seconds) = 0.00 seconds

Residual Overcurrent
50G1P Residual Overcurrent Trip Pickup (amps) = 0.5 (30A)
50G1D Residual Overcurrent Trip Delay (seconds) = 0.30 seconds

11kV Auxiliary Transformer Feeder – SEL-751A (Panel G19)
Phase CT = 40/5A 5P10 2.5VA
The recommended protection settings are provided as follows:

Phase Overcurrent
51P1P Phase Time Overcurrent Trip Pickup = 3.90 (31.2A)
51P1C TOC Curve Selection = C1 (IEC Standard Inverse)
51P1TD TOC Time Dial = 0.14

50P1P Maximum Phase Overcurrent Trip Pickup (amps) = 39.40 (315.2A)
50P1D Maximum Phase Overcurrent Trip Delay (seconds) = 0.00 seconds

Residual Overcurrent

50G1P Residual Overcurrent Trip Pickup (amps)	*= 0.5 (30A)*
50G1D Residual Overcurrent Trip Delay (seconds)	*= 0.30 seconds*

11kV Earthing Transformer Feeder – SEL-751A (Panel G20)

The earthing transformer has the following rating:

Rated Voltage	*: 11kV Rated*
Neutral Current	*: 100A Duration*
	: 10 seconds
Vector Group	*: ZN*

Phase CT = 200/5A 5P10 5VA
Neutral CT = 100/1A 5P10 15VA

The power station earthing transformer is used to limit earth fault currents to a maximum of 100 Amps on the 11kV system.

The earthing transformer protection relay should coordinate with all the feeder breakers to avoid unnecessary total blackout for faults on the mine's feeders.

With the current 11kV Switchboard configuration, the trip signal from the earthing transformer protection relay shall trip all the GCB's.

The phase overcurrent (50P and 51P) protection function is included to detect balance faults between the 11kV Switchboard and the earthing transformer and to provide fast trip with the instantaneous function. The recommended protection settings are provided as follows:

Phase Overcurrent

51P1P Phase Time Overcurrent Trip Pickup	*= 2.90 (58A)*
51P1C TOC Curve Selection	*= C1 (IEC Standard Inverse)*
51P1TD TOC Time Dial	*= 0.14*
50P1P Maximum Phase Overcurrent Trip Pickup (amps)	*= 3.00 (120A)*
50P1D Maximum Phase Overcurrent Trip Delay (seconds)	*= 0.00 seconds*

Neutral Overcurrent

50N1P Neutral Overcurrent Trip Pickup	*= 0.1 (30A)*
50N1D Neutral Overcurrent Trip Delay (seconds)	*= 0.7 seconds*

Figure 12: Protection Allows for Motor Starting

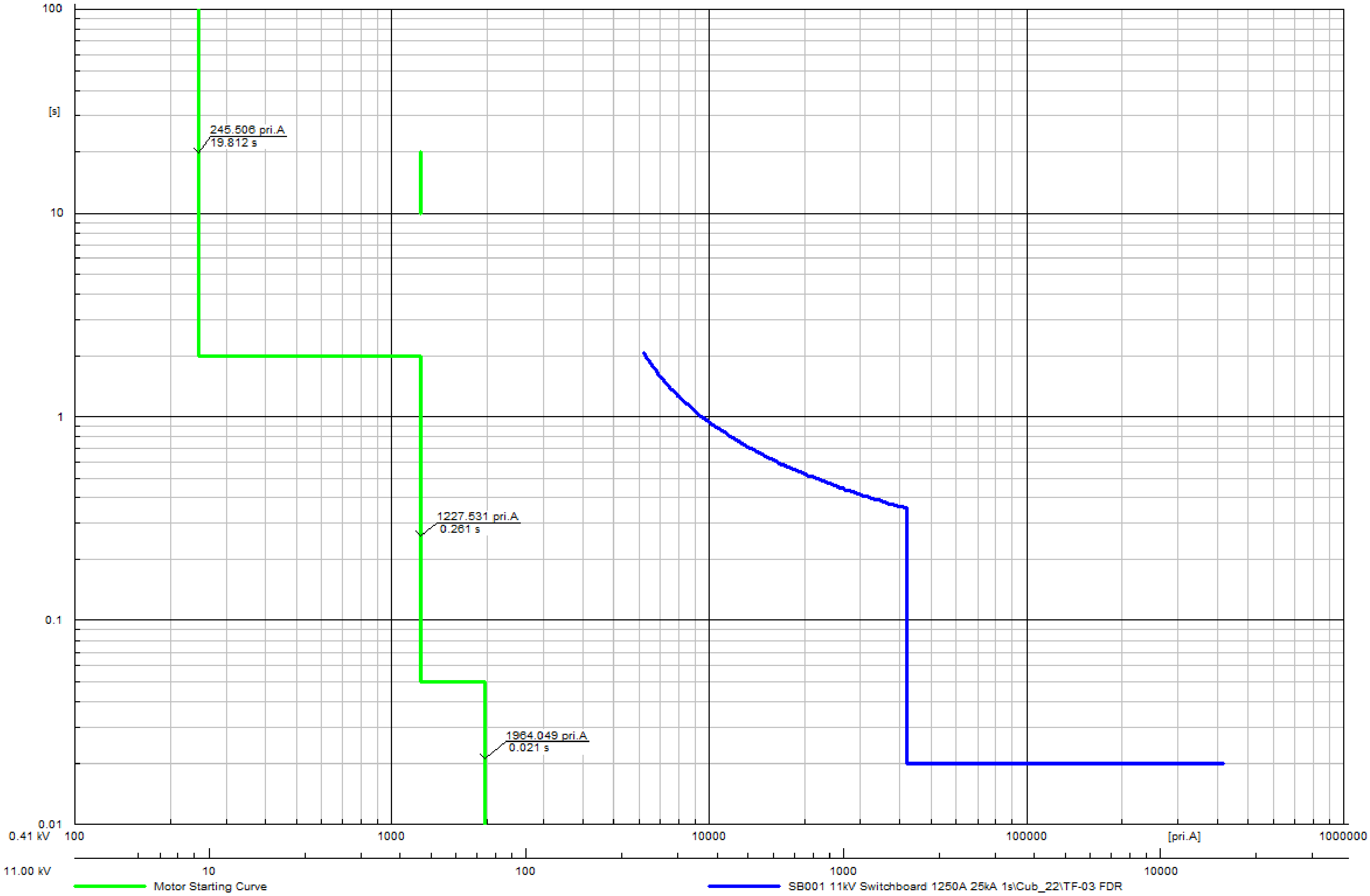

Figure 13: 3.554MVA HPGR Drive Feeders and GTCBs

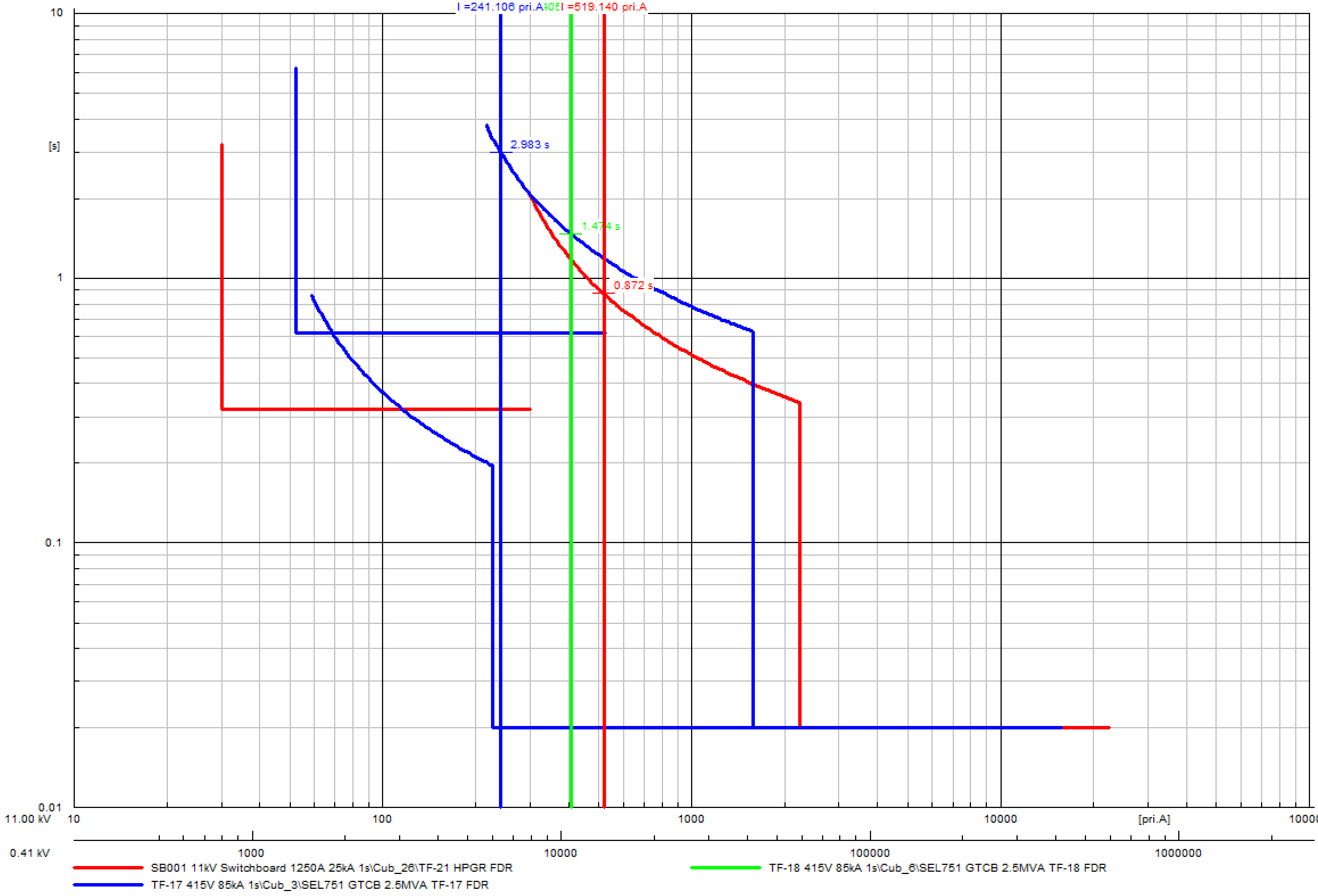

Figure 14: Auxiliary Transformer Feeder and GTCBs

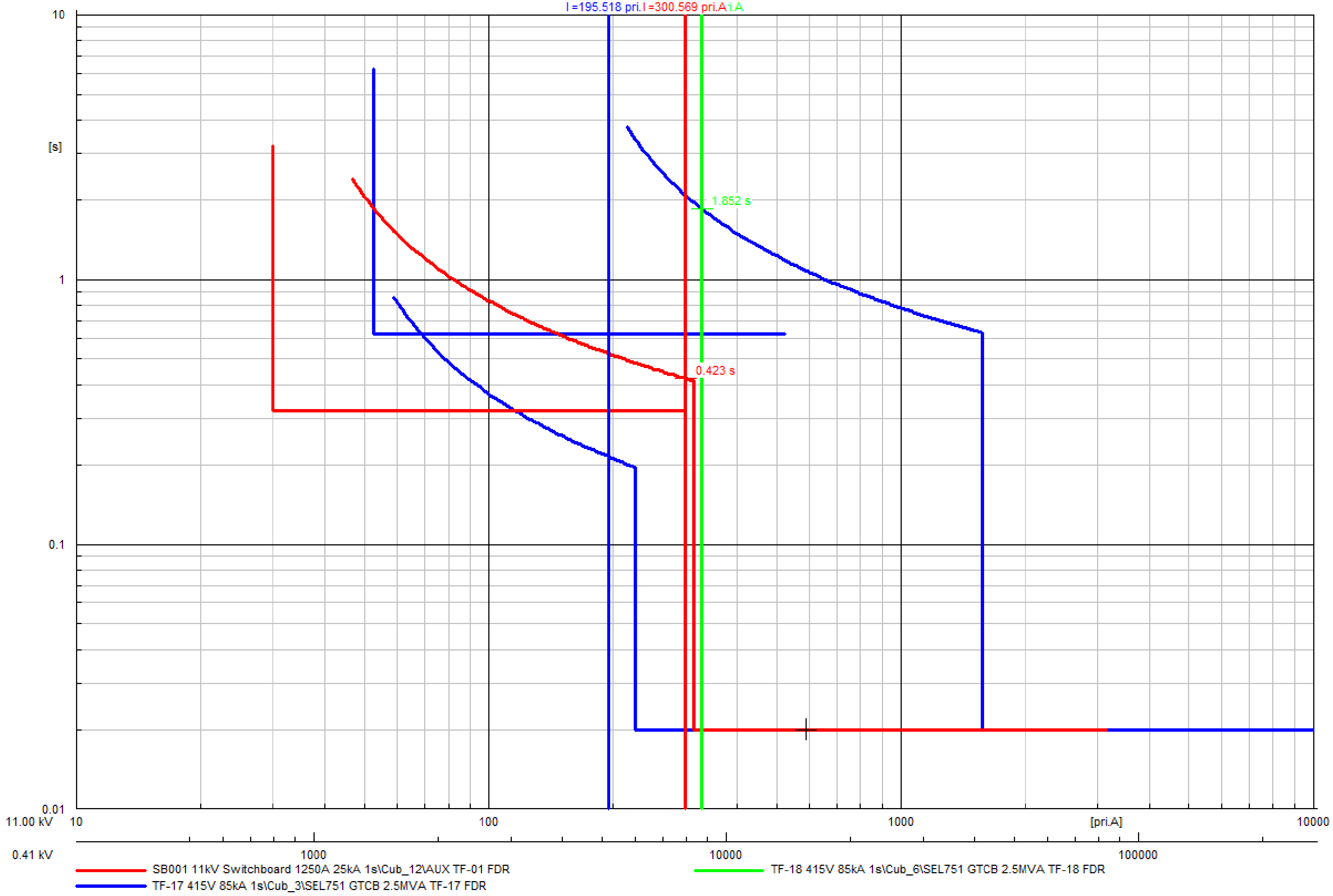

Figure 15: Earthing Transformer Feeder and GTCBs

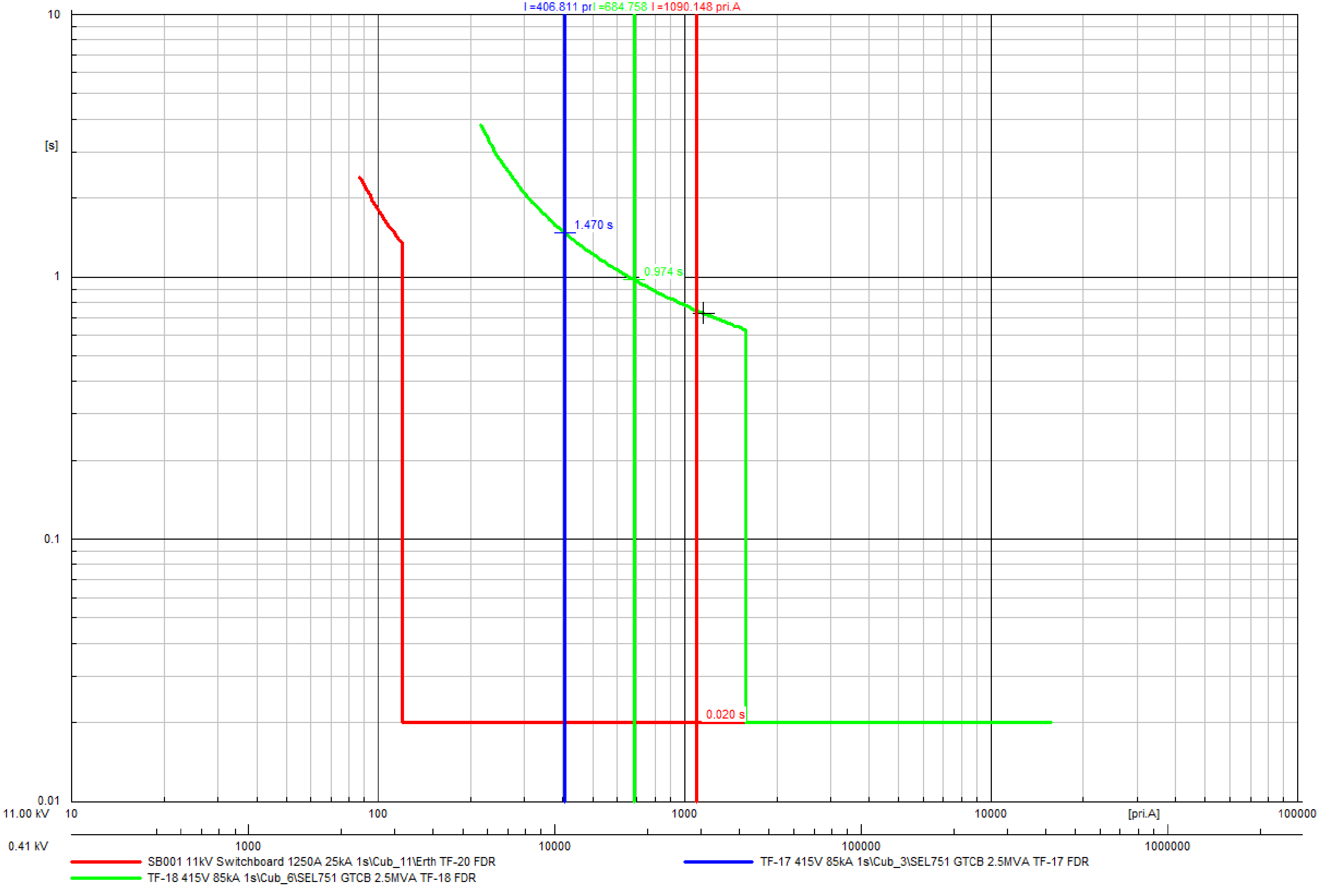

Figure 16: 2.5MVA Transformer Feeders and Earthing Transformer CB (Min Earth Fault)

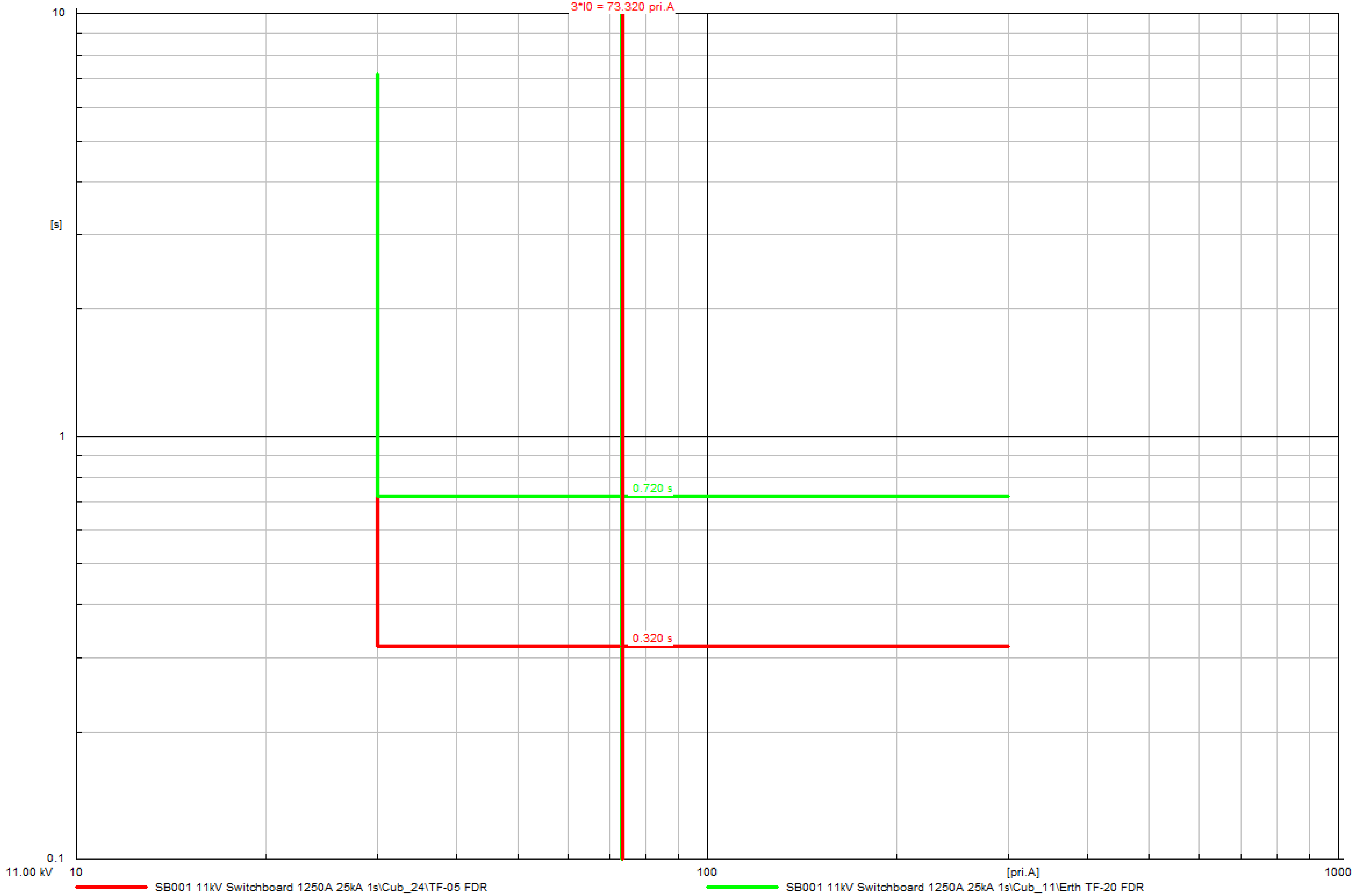

Appendix E: Motor Starting Studies

Table 30: MCC02 75kW Motor Start-Up

Bus Voltages (p.u.)			
Bus I.D.	**During Start (1.27s)**	**During Start (5s)**	**Normal Operation**
SB001	0.94	0.96	1.0
DB101	0.93	0.95	0.993
MCC-002	**0.89**	**0.93**	**0.965**
MCC-003	0.91	0.92	0.965
MCC-004	0.89	0.91	0.952
MCC-005	0.91	0.93	0.974
MCC-007	0.91	0.93	0.969

Table 31: MCC04 45kW Motor Start-Up

Bus Voltages (p.u.)			
Bus I.D.	**During Start (2.223s)**	**During Start (5s)**	**Normal Operation**
SB001	0.94	0.96	1.0
DB101	0.94	0.95	0.993
MCC-002	0.91	0.93	0.965
MCC-003	0.91	0.93	0.965
MCC-004	**0.89**	**0.91**	**0.952**
MCC-005	0.92	0.94	0.974
MCC-007	0.91	0.93	0.969

Table 32: MCC05 45kW Motor Start-Up

Bus Voltages (p.u.)			
Bus I.D.	**During Start (1.9s)**	**During Start (5s)**	**Normal Operation**
SB001	0.95	0.96	1.0
DB101	0.94	0.96	0.993
MCC-002	0.91	0.93	0.965
MCC-003	0.91	0.93	0.965
MCC-004	0.9	0.92	0.952
MCC-005	**0.91**	**0.94**	**0.974**
MCC-007	0.92	0.93	0.969

Table 33: MCC07 90kW Motor Start-Up

Bus Voltages (p.u.)			
Bus I.D.	**During Start (1.083s)**	**During Start (5s)**	**Normal Operation**
SB001	0.93	0.95	1.0
DB101	0.93	0.95	0.993
MCC-002	0.9	0.92	0.965
MCC-003	0.9	0.92	0.965
MCC-004	0.89	0.91	0.952
MCC-005	0.91	0.93	0.974
MCC-007	**0.88**	**0.92**	**0.969**

Table 34: MCC02 VSD Start-Up

Largest MCC VSD MCC02	**Normal Operation**	**Before Start**	**During Start**
Power (kW)	600	0	900
Voltage at MCC (p.u.)	0.965	0.977	0.959
Transformer Loading (%)	79.11	51.8	93.04

Table 35: MCC07 SS Start-Up

Largest MCC SS MCC07	**Normal Operation**	**Before Start**	**During Start**
Power (kW)	355	0	1065
Voltage at MCC (p.u.)	0.969	0.978	0.954
Transformer Loading (%)	65.53	47.88	94.54

Figure 17: MCC02 75kW Motor Start-Up

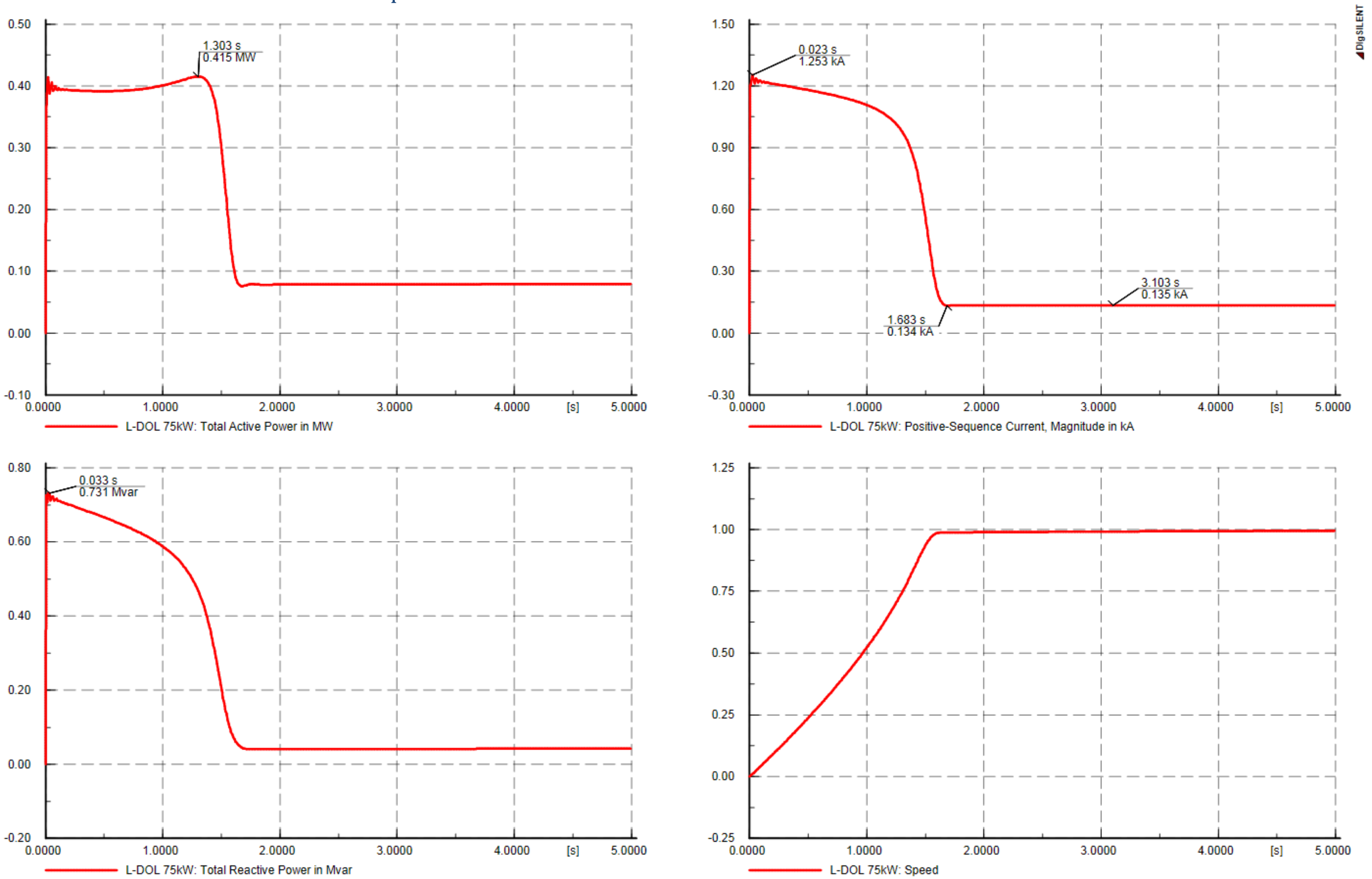

Figure 18: MCC03 150kW Motor Start-Up

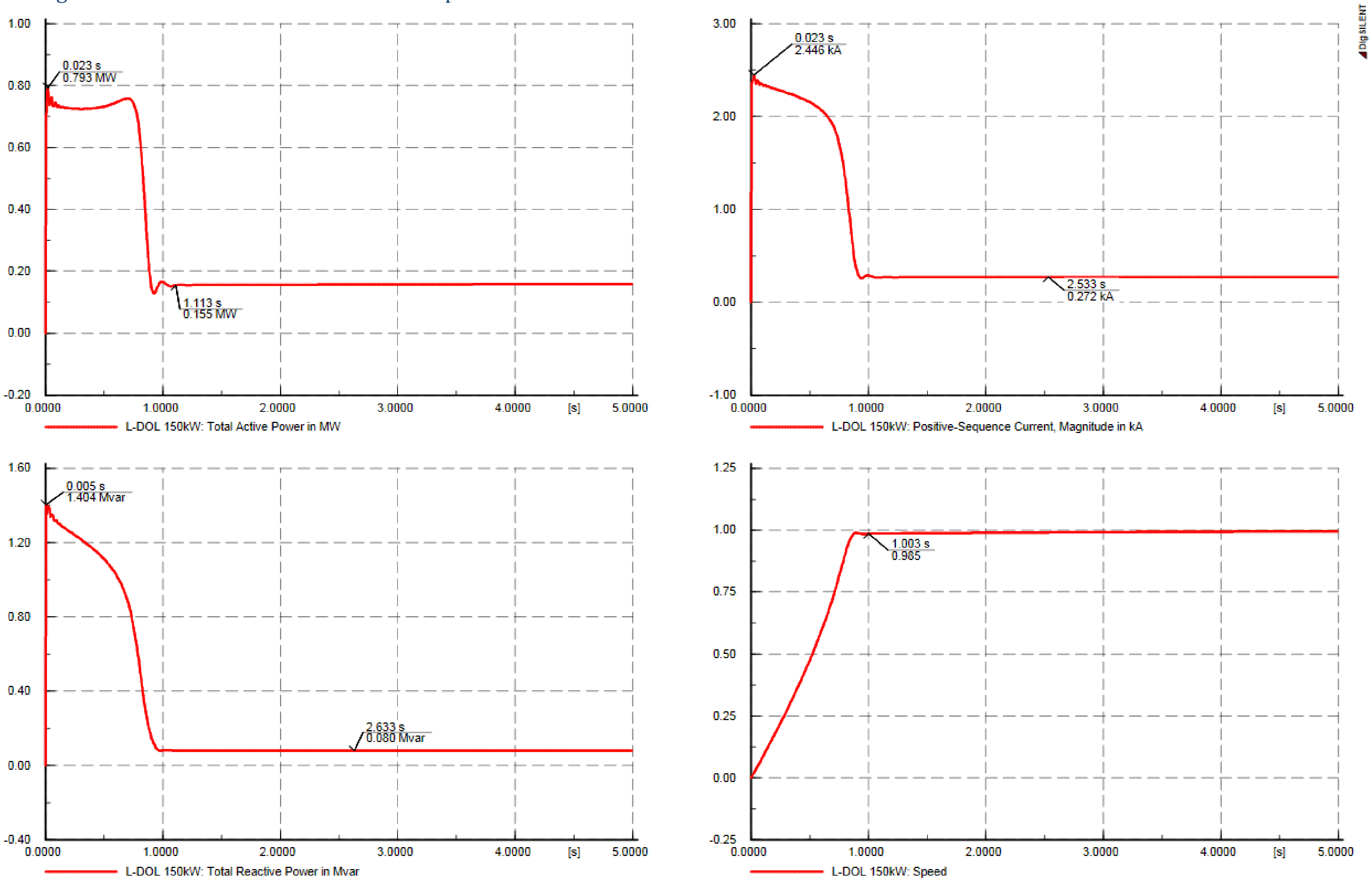

Figure 19: MCC04 45kW Motor Start-Up

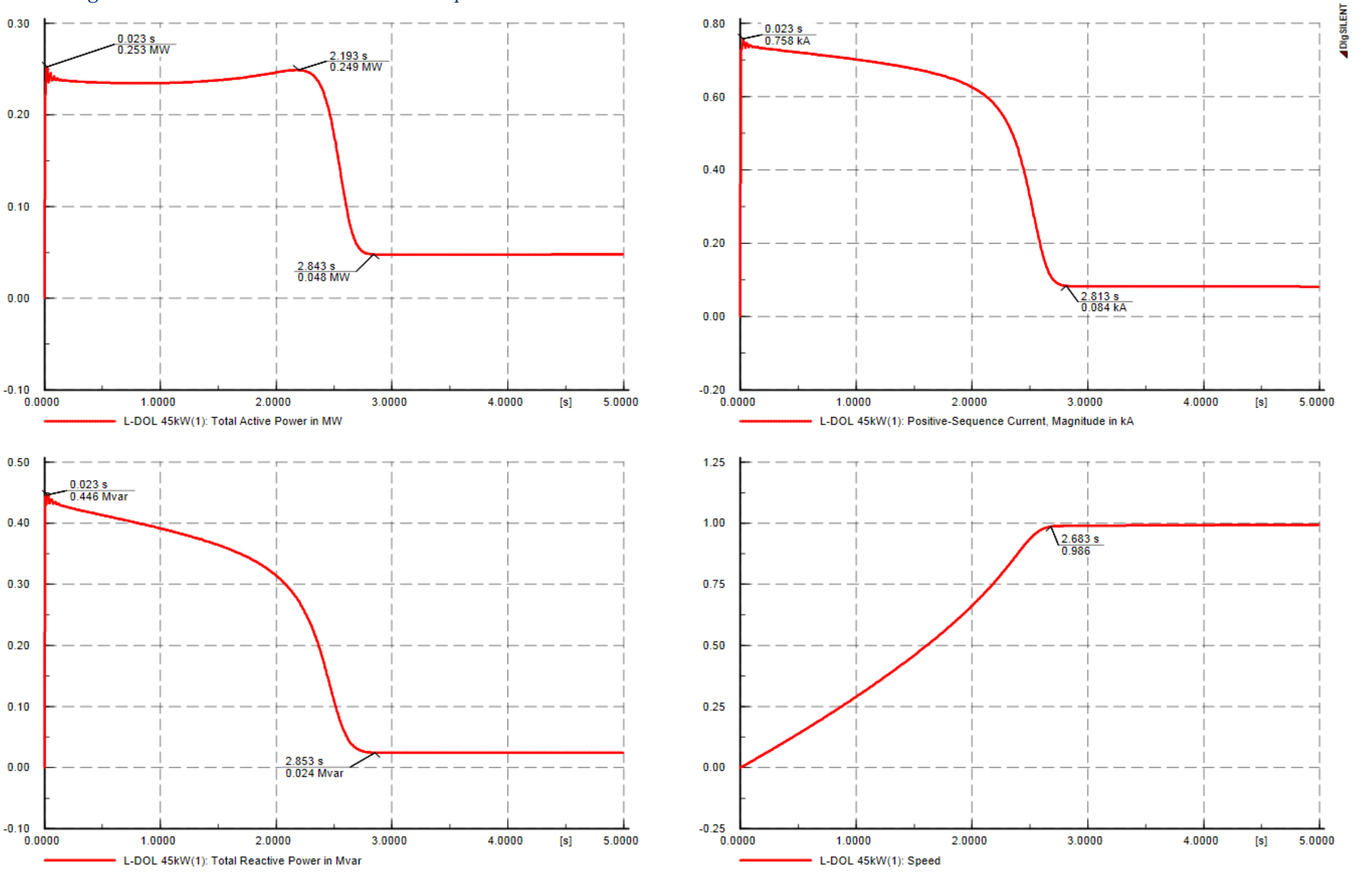

Figure 20: MCC05 45kW Motor Start-Up

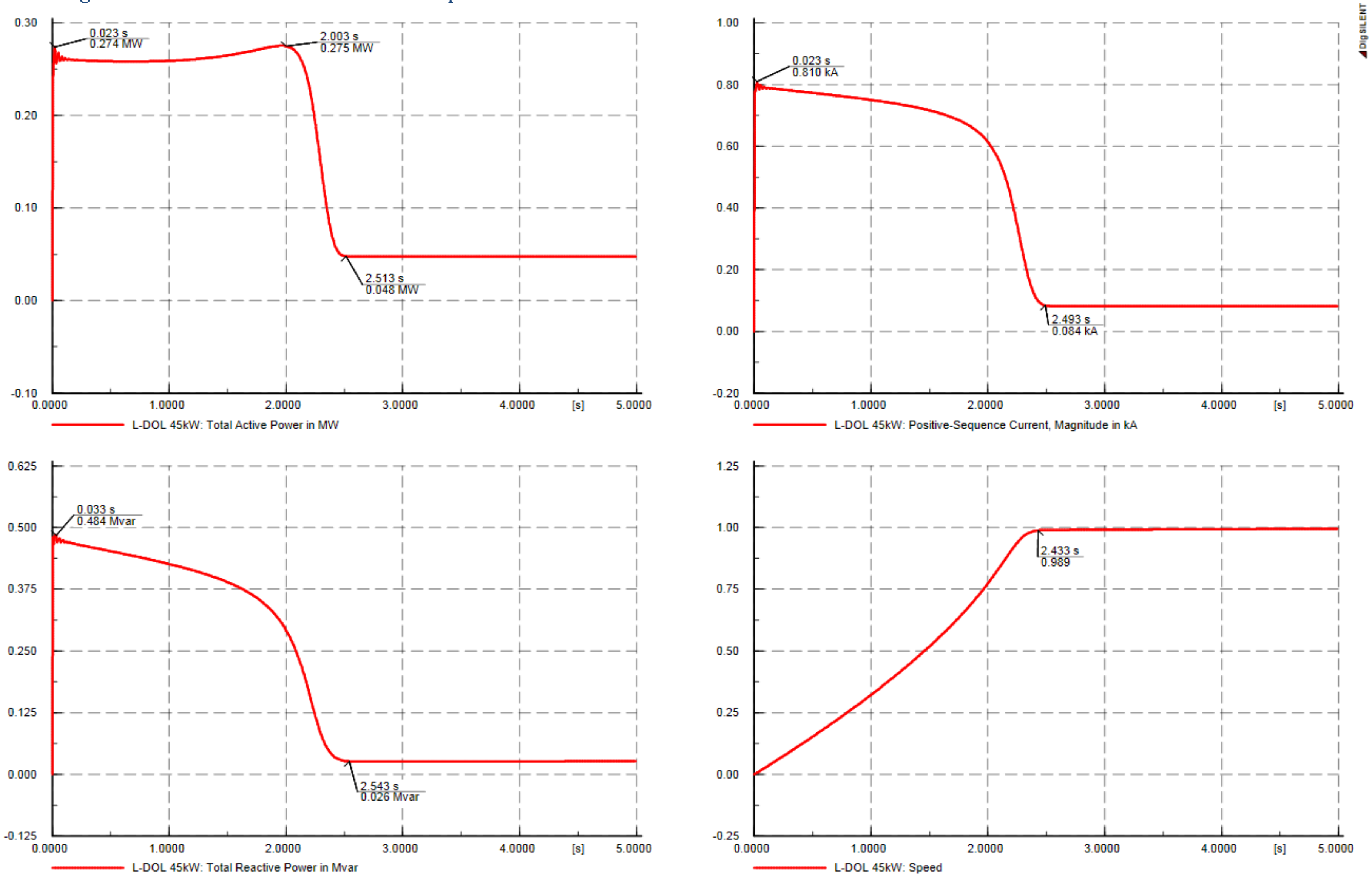

Figure 21: MCC07 90kW Motor Start-Up